

УДК 539.12.01

IMPROVED FITS TO THE xF_3 CCFR DATA
AT THE NEXT-TO-NEXT-TO-LEADING ORDER
AND BEYOND

A. L. Kataev

Institute for Nuclear Research of the Academy of Sciences of Russia, Moscow

G. Parente

Department of Particle Physics, University of Santiago de Compostela,
Santiago de Compostela, Spain

A. V. Sidorov

Joint Institute for Nuclear Research, Dubna

INTRODUCTION	44
PRELIMINARIES	46
ANOMALOUS DIMENSIONS AND COEFFICIENT FUNCTIONS: APPROXIMATE VS EXACT RESULTS	49
RESULTS OF THE FITS WITHOUT TWIST-4 TERMS	53
INCORPORATION OF THE TWIST-4 TERMS	57
Infrared Renormalon Model Parameterization	57
IRR Approach and Naive Non-Abelianization	60
The Determination of $\alpha_s(M_Z)$ Values and Their Scale- Dependence Uncertainties	64
Determination of the x Shape of the Twist-4 Corrections	72
COMPARISON WITH THE RESULTS OF OTHER NNLO ANALYSES	75
Comments on Estimates of Scale-Scheme Dependence Un- certainties	76
Comments on Outputs of the NNLO Bernstein Polynomial Analyses	79
The Model Independence of High-Twist Duality Effect	82
CONCLUSIONS	83
Acknowledgements	84
REFERENCES	84

УДК 539.12.01

IMPROVED FITS TO THE xF_3 CCFR DATA AT THE NEXT-TO-NEXT-TO-LEADING ORDER AND BEYOND

A. L. Kataev

Institute for Nuclear Research of the Academy of Sciences of Russia, Moscow

G. Parente

Department of Particle Physics, University of Santiago de Compostela,
Santiago de Compostela, Spain

A. V. Sidorov

Joint Institute for Nuclear Research, Dubna

A review of the analysis of Tevatron data for xF_3 structure function of deep inelastic νN scattering, provided by CCFR collaboration, is presented. Special attention is paid to taking into account of the higher-order perturbative QCD effects and nonperturbative contributions. Using the results for the NNLO QCD corrections to anomalous dimensions of odd xF_3 Mellin moments and N³LO corrections to their coefficient functions we improve previous analysis of the CCFR'97 data for xF_3 . The possibility of extracting the $1/Q^2$ -corrections from the fits is analysed using three independent models. Theoretical question of applicability of the renormalon-type inspired large- β_0 approximation for estimating corrections to the coefficient functions of odd xF_3 and even nonsinglet F_2 moments is considered. The comparison with [1/1] Padé estimates is given. The obtained NNLO values of $\alpha_s(M_Z)$ are in agreement with the world average value $\alpha_s(M_Z) \approx 0.118$. We also present the first N³LO extraction of $\alpha_s(M_Z)$. The interplay between higher-order perturbative QCD corrections and $1/Q^2$ -terms is demonstrated. The results of our studies are compared with those obtained recently using the NNLO model of the kernel of the DGLAP equation and with the results of the NNLO fits to CCFR'97 xF_3 data, performed by the Bernstein polynomial technique.

Приведен анализ данных для структурной функции xF_3 глубоконеупругого νN -рассеяния, полученных на тэватроне коллаборацией CCFR. Особое внимание уделено учету высших поправок теории возмущений КХД и вкладам эффектов, возникающих вне рамок теории возмущений. Используя результаты вычислений трехпетлевых поправок к аномальным размерностям нечетных моментов Меллина от xF_3 и вкладов более высокого порядка теории возмущений к их коэффициентным функциям, мы детализируем наши предыдущие работы, посвященные обработке данных коллаборации CCFR для xF_3 . В рамках трех независимых моделей проанализирована возможность извлечения из фитов поправок порядка $1/Q^2$. Рассмотрены теоретические особенности применимости ренормального подхода для оценок высших поправок теории возмущений к коэффициентным функциям нечетных моментов от xF_3 и четных моментов от несинглетной части структурной функции F_2 . Проведено сравнение с результатами применения техники диагональных [1/1] аппроксимантов Падэ. Полученное в результате фитов трехпетлевое значение константы связи КХД $\alpha_s(M_Z)$ находится в хорошем согласии с ее среднемировым значением

$\alpha_s(M_Z) \approx 0,118$. Впервые проведено извлечение значения $\alpha_s(M_Z)$ в четырехпетлевом приближении. Продемонстрирована корреляция между высшими поправками теории возмущений и вкладами степенных членов, подавленных $1/Q^2$. Приведено сравнение результатов нашего анализа для $\alpha_s(M_Z)$ с аналогичными результатами других работ, в которых использовались приближенное трехпетлевое ядро уравнения Докшитцера–Грибова–Липатова–Алтарелли–Паризи и метод полиномов Бернштейна.

INTRODUCTION

The series of our previous works [1–5] (for a brief summary, see the review of Ref. 6) was devoted to the QCD analysis of the xF_3 data obtained at the Fermilab Tevatron. In Refs. 3–5, we made the consequent steps towards the next-to-next-to-leading order (NNLO) fits to the xF_3 CCFR’97 data [7] both without and with twist-4 corrections taken into account. In the process of these studies, definite theoretical approximations were made. Let us recall the basic steps of these studies.

The x behaviour of xF_3 was reconstructed from the Mellin moments with the number $2 \leq n \leq 10$ with the help of the Jacobi polynomial technique, developed in Refs. 8–12. At the NNLO, the perturbative expansion for the coefficient functions of these moments is explicitly known from analytical calculations of Refs. 13, which were confirmed recently with the help of another technique [14]. However, the NNLO corrections to the anomalous dimensions of the considered nonsinglet (NS) moments, closely related to still analytically unknown NNLO contributions to the kernel of the DGLAP equation [15–18], were modelled in the definite approximations only. These approximations were based on the observation that for $2 \leq n \leq 10$ the next-to-leading (NLO) corrections to the anomalous dimensions $\gamma_{\text{NS},F_2}^{(1)}(n)$ of the NS Mellin moments for F_2 do not numerically differ from the NLO corrections to the anomalous dimensions $\gamma_{F_3}^{(1)}(n)$ of the moments taken from the xF_3 structure function (SF) [1]. In view of this it was assumed that this similarity will be true in the case of higher-order corrections to the anomalous dimensions $\gamma_{\text{NS},F_2}^{(n)}$ and $\gamma_{F_3}^{(n)}$ as well, provided the typical diagrams with new Casimir structure $d^{abc}d^{abc}$ (which are starting to contribute to $\gamma_{F_3}^{(n)}$ from the NNLO) are not large. Using this assumption, we applied in our analysis [3–5] of the xF_3 CCFR’97 data [7] the available results for the NNLO corrections to $\gamma_{\text{NS},F_2}^{(2)}(n)$, which were known in the cases of $n = 2, 4, 6, 8, 10$ due to the distinguished calculations of Refs. 19, 20. For the odd moments with $n = 3, 5, 7, 9$, the NNLO corrections to $\gamma_{\text{NS},F_2}^{(2)}(n)$ were estimated using the procedure of smooth interpolations, previously proposed in Ref. 21 in the process of the first NS NNLO fits to the F_2 data of the BCDMS collaboration [22].

Quite recently the renormalization group quantities for the xF_3 Mellin moments were analytically calculated at the NNLO level [23] by the methods of

Refs.24–26, used in the case of calculations of the even Mellin moments of F_2 [19,20]. In Ref.23, the following information, quite useful for the improvement of the previous fits, was obtained:

the NNLO corrections to $\gamma_{F_3}^{(n)}$ at $n = 3, 5, 7, 9, 11, 13$;

the NNLO corrections to $\gamma_{NS,F_2}^{(n)}$ at $n = 12$ and $n = 14$;

the N³LO corrections to the coefficient functions of odd Mellin moments of xF_3 with $n = 3, 5, 7, 9, 11, 13$ *.

Due to the appearance of this new important information, it became possible to recast the analysis of Refs.3–5 on a new level of understanding. First, we are now able to increase the precision of the smooth interpolation procedure for $\gamma_{NS,F_2}^{(n)}$, applied in the process of the works of Refs.1–5. Second, it is now possible to change the previously-used approximation for NS anomalous dimensions and take into account the available expressions for the NNLO corrections to $\gamma_{F_3}^{(n)}$ including terms typical to this level of perturbation theory, which are proportional to $f(d^{abc}d^{abc})/n$ (in our case we will consider $f = 4$ number of massless active flavours, while for the $SU_C(3)$ -group $(d^{abc}d^{abc})/3 = 40/9$). Moreover, since the best way of estimating the perturbative part of theoretical uncertainties of the N⁽ⁱ⁾LO fits is the incorporation of the N⁽ⁱ⁺¹⁾LO-terms, the results of Ref.23 give us the chance to perform the approximate N³LO analysis of xF_3 data and compare its outcome with the results obtained within the framework of the N³LO Padé motivated fits of Ref.5.

The aims of this work are the following:

1. To present a description of the NNLO analysis of Tevatron data for xF_3 , eliminating theoretical uncertainties related to the previously-used NNLO approximation $\gamma_{NS,F_2}^{(2)}(n) \approx \gamma_{F_3}^{(2)}(n)$ at $2 \leq n \leq 10$;

2. To include in the analysis the NNLO corrections to the coefficient functions $C_{F_3}^{(n)}$ and to the anomalous dimensions $\gamma_{F_3}^{(n)}$ up to $n \leq 13$ (the first results of this program were already presented in Ref.28);

3. To study, in more detail, the feature of the interplay between NNLO perturbative QCD corrections and $1/Q^2$ -terms, discovered in Refs.3, 5, which leads to the effective decrease of the value of the basic free parameter of the infrared renormalon (IRR) model for the twist-4 contribution to xF_3 [29] (for the discussions of the IRR contributions to characteristics of deep inelastic scattering, see Refs.30, 31, while for recent reviews of the current general status of the IRR approach, see Refs.32, 33);

4. To comment upon the predictive abilities and special features of the Padé approximants at the N³LO level;

*In the case of $n = 1$, the α_s^3 contribution to the Gross–Llewellyn-Smith sum rule was already known [27].

5. To study the applicability of the renormalon-inspired large- β_0 expansion for estimating higher-order perturbative corrections to the coefficient functions of moments of xF_3 , which will be used by us. The similar consideration of NS moments for F_2 SF [34] is also updated. The results will be compared with those obtained by means of the Padé approximation technique;

6. To study the scale-dependence of the obtained values for α_s at the NLO and beyond;

7. To reconsider the problem of the extraction of the x -shape of the twist-4 contributions at the LO, NLO, NNLO using new information about $\gamma_{F_3}^{(2)}(n)$ and taking into account additional terms in the perturbative expansion of $C_{F_3}^{(n)}$ at the N³LO;

8. To compare our results with other phenomenological applications of the perturbative QCD calculations of Refs. 13, 23, which appeared in the literature recently and were based on the application of DGLAP approach (see Ref. 35) and Bernstein polynomial technique proposed in Ref. 36 and used at the NNLO in Ref. 37.

It should be stressed that, since in the current work we are interested in the study of *theoretical ambiguities* of the outcome of the fits on a more solid background than was done in Ref. 5 and in revealing *the importance* of the knowledge of *exact expressions* for still uncalculated NNLO corrections to $\gamma_{F_3}^{(2)}(n)$ for n even, we will neglect the systematic experimental uncertainties of the CCFR'97 xF_3 data, taking into account statistical ones only. The incorporation of systematic error-bars into the fits might shadow the effects of fixing the theoretical uncertainties we are struggling for and might make the process of clarification of the necessity of getting explicit numbers for $\gamma_{F_3}^{(2)}(n)$ for even n more complicated. At the NLO level the combined analysis of statistical and systematic experimental uncertainties of the xF_3 CCFR'97 data was done in Refs. 38, 39 using the machinery of the method proposed in Ref. 40.

1. PRELIMINARIES

For the sake of completeness of the presentation, we will repeat some definitions from Ref. 5.

We start from the Mellin moments for $xF_3(x, Q^2)$:

$$M_n^{F_3}(Q^2) = \int_0^1 x^{n-1} F_3(x, Q^2) dx, \quad (1)$$

where $n = 2, 3, 4, \dots$. These moments obey the following renormalization group

equation

$$\left(\mu \frac{\partial}{\partial \mu} + \beta(A_s) \frac{\partial}{\partial A_s} - \gamma_{F_3}^{(n)}(A_s) \right) M_n^{F_3}(Q^2/\mu^2, A_s(\mu^2)) = 0, \quad (2)$$

where $A_s = \alpha_s/(4\pi)$. The renormalization group functions are defined as

$$\begin{aligned} \mu \frac{\partial A_s}{\partial \mu} = \beta(A_s) = -2 \sum_{i \geq 0} \beta_i A_s^{i+2} - \\ - \mu \frac{\partial \ln Z_n^{F_3}}{\partial \mu} = \gamma_{F_3}^{(n)}(A_s) = \sum_{i \geq 0} \gamma_{F_3}^{(i)}(n) A_s^{i+1}. \end{aligned} \quad (3)$$

The NS anomalous dimensions of F_2 will be defined in the analogous way, namely:

$$- \mu \frac{\partial \ln Z_n^{\text{NS}, F_2}}{\partial \mu} = \gamma_{\text{NS}, F_2}^{(n)}(A_s) = \sum_{i \geq 0} \gamma_{\text{NS}, F_2}^{(i)}(n) A_s^{i+1}, \quad (4)$$

where $Z_n^{F_3}$ and Z_n^{NS, F_2} are the renormalization constants of the corresponding NS operators. In the case of xF_3 moments, the solution of the renormalization group equation is:

$$\frac{M_n^{F_3}(Q^2)}{M_n^{F_3}(Q_0^2)} = \exp \left[- \int_{A_s(Q_0^2)}^{A_s(Q^2)} \frac{\gamma_{F_3}^{(n)}(x)}{\beta(x)} dx \right] \frac{C_{F_3}^{(n)}(A_s(Q^2))}{C_{F_3}^{(n)}(A_s(Q_0^2))}, \quad (5)$$

where $M_n^{F_3}(Q_0^2)$ is a phenomenological quantity defined at the initial scale Q_0^2 as:

$$M_n^{F_3}(Q_0^2) = \int_0^1 x^{n-2} A(Q_0^2) x^{b(Q_0^2)} (1-x)^{c(Q_0^2)} (1 + \gamma(Q_0^2)x) dx. \quad (6)$$

This expression is identical to the parametrization used by the CCFR collaboration [7]. In the process of our studies we will extract from the fits the parameters $A(Q_0^2)$, $b(Q_0^2)$, $c(Q_0^2)$, and $\gamma(Q_0^2)$, together with the parameter $\Lambda_{\overline{MS}}^{(4)}$ and with the information on the twist-4 terms.

The first moment of xF_3 coincides with the Gross–Llewellyn-Smith sum rule

$$\text{GLS}(Q^2) = M_1^{F_3}(Q^2) = \int_0^1 F_3(x, Q^2) dx. \quad (7)$$

At the N³LO the coefficient function $C_{F_3}^{(n)}$, which enters Eq. (5), can be defined as

$$C_{F_3}^{(n)}(A_s) = 1 + C_{F_3}^{(1)}(n) A_s + C_{F_3}^{(2)}(n) A_s^2 + C_{F_3}^{(3)}(n) A_s^3, \quad (8)$$

while the corresponding expression for the anomalous-dimension term is:

$$\exp \left[- \int^{A_s(Q^2)} \frac{\gamma_{F_3}^{(n)}(x)}{\beta(x)} dx \right] = (A_s(Q^2))^{\gamma_{F_3}^{(0)}(n)/2\beta_0} \times AD(n, A_s), \quad (9)$$

where

$$AD(n, A_s) = [1 + p(n)A_s(Q^2) + q(n)A_s(Q^2)^2 + r(n)A_s(Q^2)^3] \quad (10)$$

and $p(n)$, $q(n)$, and $r(n)$ read:

$$p(n) = \frac{1}{2} \left(\frac{\gamma_{F_3}^{(1)}(n)}{\beta_1} - \frac{\gamma_{F_3}^{(0)}(n)}{\beta_0} \right) \frac{\beta_1}{\beta_0}, \quad (11)$$

$$q(n) = \frac{1}{4} \left(2p(n)^2 + \frac{\gamma_{F_3}^{(2)}(n)}{\beta_0} + \gamma_{F_3}^{(0)}(n) \frac{(\beta_1^2 - \beta_2\beta_0)}{\beta_0^3} - \gamma_{F_3}^{(1)}(n) \frac{\beta_1}{\beta_0^2} \right), \quad (12)$$

$$r(n) = \frac{1}{6} \left(-2p(n)^3 + 6p(n)q(n) + \frac{\gamma_{F_3}^{(3)}(n)}{\beta_0} - \frac{\beta_1\gamma_{F_3}^{(2)}(n)}{\beta_0^2} - \frac{\beta_2\gamma_{F_3}^{(1)}(n)}{\beta_0^2} + \frac{\beta_1^2\gamma_{F_3}^{(1)}(n)}{\beta_0^3} - \frac{\beta_1^3\gamma_{F_3}^{(0)}(n)}{\beta_0^4} - \frac{\beta_3\gamma_{F_3}^{(0)}(n)}{\beta_0^2} + \frac{2\beta_1\beta_2\gamma_{F_3}^{(0)}(n)}{\beta_0^3} \right). \quad (13)$$

The coupling constant $A_s(Q^2)$ can be decomposed into the inverse powers of $L = \ln(Q^2/\Lambda_{MS}^2)$ as $A_s^{\text{NLO}} = A_s^{\text{LO}} + \Delta A_s^{\text{NLO}}$, $A_s^{\text{NNLO}} = A_s^{\text{NLO}} + \Delta A_s^{\text{NNLO}}$ and $A_s^{\text{N}^3\text{LO}} = A_s^{\text{NNLO}} + \Delta A_s^{\text{N}^3\text{LO}}$, where

$$A_s^{\text{LO}} = \frac{1}{\beta_0 L}, \quad \Delta A_s^{\text{NLO}} = -\frac{\beta_1 \ln(L)}{\beta_0^3 L^2}, \quad (14)$$

$$\Delta A_s^{\text{NNLO}} = \frac{1}{\beta_0^5 L^3} [\beta_1^2 \ln^2(L) - \beta_1^2 \ln(L) + \beta_2\beta_0 - \beta_1^2], \quad (15)$$

$$\Delta A_s^{\text{N}^3\text{LO}} = \frac{1}{\beta_0^7 L^4} \left[\beta_1^3 \left(-\ln^3(L) + \frac{5}{2} \ln^2(L) + 2 \ln(L) - \frac{1}{2} \right) - 3\beta_0\beta_1\beta_2 \ln(L) + \beta_0^2 \frac{\beta_3}{2} \right]. \quad (16)$$

Notice that in our normalization the expressions for β_0 , β_1 , β_2 , and β_3 have the following numerical expressions:

$$\begin{aligned}
\beta_0 &= 11 - 0.6667f, \\
\beta_1 &= 102 - 12.6667f, \\
\beta_2 &= 1428.50 - 279.611f + 6.01852f^2, \\
\beta_3 &= 29243.0 - 6946.30f + 405.089f^2 + 1.49931f^3,
\end{aligned}
\tag{17}$$

where β_2 is known from calculations of Ref. 41 and β_3 was analytically calculated in Ref. 42.

2. ANOMALOUS DIMENSIONS AND COEFFICIENT FUNCTIONS: APPROXIMATE VS EXACT RESULTS

Let us discuss the numerical approximations of higher-order perturbative corrections to anomalous dimensions and coefficient functions, used in our fits. The analytical expression for the one-loop term of NS anomalous dimensions $\gamma_{\text{NS},F_2}^{(0)}(n) = \gamma_{F_3}^{(0)}(n) = 8/3[4\sum_{j=1}^n(1/j) - 2/n(n+1) - 3]$ is well known. The NLO corrections to the NS anomalous dimensions were obtained in Refs. 43, 44 and confirmed by the independent calculation in Ref. 45. In the cases of both F_2 and xF_3 , the numerical expressions for the NLO contributions to the anomalous dimensions are given in Table 1, where we also present the numerical values of the NNLO coefficients used in the NS anomalous-dimension functions of Eqs. (3) and (4). They are also normalized to the case of $f = 4$ number of flavours. The coefficients $\gamma_{F_3}^{(2)}(n)|_{wts}$ represent the contribution to $\gamma_{F_3}^{(2)}$ of the terms without typical structure (*wts*) $f(d^{abc}d^{abc})/n = 4 * 40/9$, which is absent in the expression for $\gamma_{\text{NS},F_2}^{(2)}$ and appears for the first time in the anomalous dimensions of xF_3 moments at the NNLO.

We describe now how the related approximations for $\gamma_{\text{NS},F_2}^{(2)}(n)$ and $\gamma_{F_3}^{(2)}(n)$ were obtained and what is the connection between the sets of these numbers. The expressions without round brackets are the results of explicit analytical calculations of Refs. 19, 20, 23. The expressions in round brackets are the approximations obtained with the help of the smooth interpolation procedure. To study the possibility of getting stable dependence of the values for $\Lambda_{\overline{MS}}^{(4)}$ on the change of the initial scale Q_0^2 after incorporation into the fits of the NNLO corrections to $\gamma_{F_3}^{(n)}$ with $10 < n < 13$, the interpolation procedure was supplemented with the fine tuning of the NNLO corrections to $\gamma_{F_3}^{(2)}(n)$ with $n = 6, 8, 10$.

The numerical values of the obtained fine-tuned numbers will be given in the next Section. This procedure results in better stability of the fitted values of

Table 1. The numerical expressions for NLO and NNLO coefficients of anomalous dimensions of NS moments of F_2 and $x F_3$ at $f = 4$ number of flavours

n	$\gamma_{\text{NS},F_2}^{(1)}(n)$	$\gamma_{F_3}^{(1)}(n)$	$\gamma_{\text{NS},F_2}^{(2)}(n)$	$\gamma_{F_3}^{(2)}(n) _{wts}$	$\gamma_{F_3}^{(2)}(n)$
2	71.374	71.241	612.0598	(585)	(631)
3	100.801	100.782	(839.8534)	836.3440	861.6526
4	120.145	120.140	1005.823	(1001.418)	(1015.368)
5	134.905	134.903	(1134.967)	1132.727	1140.900
6	147.003	147.002	1242.0006	(1241.21)	(1246.59)
7	157.332	157.332	(1334.865)	1334.316	1338.272
8	166.386	166.386	1417.451	(1416.73)	(1419.783)
9	174.468	174.468	(1491.711)	1491.124	1493.466
10	181.781	181.781	1559.005	(1558.854)	(1560.675)
11	188.466	188.466	(1620.755)	1620.727	1622.283
12	194.629	194.629	1678.400	(1677.696)	(1679.809)
13	200.350	200.350	(1732.640)	1731.696	1732.809

$\Lambda_{\overline{MS}}^{(4)}$ with respect to changes of the initial scale at $Q_0^2 \geq 5 \text{ GeV}^2$ (see Table 4 below). The approximation for $\gamma_{F_3}^{(2)}(2)$ contains more uncertainties. At the first stage it was obtained by extrapolation of the NNLO coefficients to anomalous dimensions with $n > 2$ without using an explicit number for $\gamma_{F_3}^{(2)}(n = 1)$ (which is zero). We have checked the reliability of this procedure, considering the set of NLO anomalous dimensions $\gamma_{F_3}^{(1)}(n)$ which are explicitly known at any values of n . We found that the interpolated values at even $n = 4, 6, \dots$ are much closer to the real numbers than those obtained with incorporation of the zero expression for the $n = 1$ anomalous dimension. In this case, for $n = 2$ we obtained the extrapolated value (75.41), which is over 6% higher than the real value 71.24. In the case of application of the interpolation procedure, which used the $n = 1$ result (zero), we get the value (66.11), which is 6% smaller than the real value. To estimate the NNLO expression for $\gamma_{F_3}^{(2)}(2)$ we imposed the conditions of the reduction found at the NLO and thus fixed the value of $\gamma_{F_3}^{(2)}(2)$ 6% below the extrapolated number. Its numerical expression, which will be used throughout this work, is quoted in Table 1. The 6% uncertainty of $\gamma_{F_3}^{(2)}(2)$ translates to a 1–2 MeV variation of $\Lambda_{\overline{MS}}^{(4)}$, which is below the precision of the NNLO extraction of the value of this parameter.

In view of the doubts of the validity of the interpolation procedure, expressed in Ref. 46, it is of definite interest to describe the results of its applications in more detail. At the first stage, one can compare the interpolated numerical expressions for $\gamma_{\text{NS},F_2}^{(2)}(n)$ at $n = 3, 5, 7, 9, 11, 13$, obtained with application of values recently

calculated in Ref. 23 for $\gamma_{\text{NS},F_2}^{(2)}(12)$ and $\gamma_{\text{NS},F_2}^{(2)}(14)$ with the explicit identical results for $\gamma_{F_3}^{(2)}(n)|_{wts}$, which do not contain the $d^{abc}d^{abc}$ -structure. The comparison is presented in Table 1. The estimates from the third column (839.8534), (1134.967), (1334.865), (1491.711), (1620.755), (1732.640) should be compared with the explicit numbers 836.3440; 1132.727; 1334.316; 1491.124; 1620.727, and 1731.696. One can see that the qualitative agreement between these sets of numbers is rather good. Moreover, we can study the applicability of the interpolation procedure for simulating explicitly unknown coefficients of $\gamma_{\text{NS},F_2}^{(2)}(n)$ obtained with and without application of $\gamma_{\text{NS},F_2}^{(2)}(12)$ and $\gamma_{\text{NS},F_2}^{(2)}(14)$ terms. In fact we found that for $n = 3, 5, 7, 9$ the difference between the «new» and «old» interpolated numbers is not large, namely 2.45; -0.8 ; 0.9; -1.8 . It affects the third significant digit of the interpolated estimates and improves their qualitative agreement with the results of the calculations of $\gamma_{F_3}^{(2)}(n)$ at odd values of n [23]. However, it is known that even a knowledge of the 3rd significant digit in anomalous-dimension terms is not enough for the precise reconstruction of SF from the NLO results for the moments at large $n \geq 6$ [11, 12]. Therefore, to determine the unknown even values of $\gamma_{\text{NS},F_3}^{(2)}(n)$ from the known NNLO corrections to $\gamma_{F_3}^{(2)}(n)$ at $n = 3, 5, 7, 9, 11, 13$ [23] with more precision, we supplement the interpolation procedure for $\gamma_{F_3}^{(2)}(n)$ by the fine-tuning of its terms for $n = 6, 8, 10$. The results of the application of the first approximation are presented in the last column of Table 1. Notice that they contain the scheme-independent new contributions, labelled by the $d^{abc}d^{abc}$ gauge group structure. The fine-tuned expressions for $\gamma_{F_3}^{(2)}(n)$ at $n = 6, 8, 10$ will be presented below.

One more verification of the idea of smooth interpolation comes from the consideration of its application for estimating NNLO corrections to the coefficient functions of even Mellin moments of xF_3 . The estimates obtained are presented in column 4 of Table 2. The comparison with the results given in column 3, which were calculated from the expression of Ref. 13, demonstrates perfect agreement of these estimates with the explicit numbers. We think that, in view of this, one can safely apply the idea of smooth interpolation in order to estimate the N³LO terms to the coefficient functions of even Mellin moments of xF_3 from those calculated in Ref. 23 with $n = 3, 5, 7, 9, 11, 13$, and also taking into account the order $O(A_s^3)$ correction to the Gross–Llewellyn–Smith sum rule ($n = 1$ moment), obtained in Ref. 27.

The information about the N³LO corrections to the considered coefficient functions is the important and dominating ingredient of the N³LO fits to xF_3 data we are going to perform. It should be supplemented with the model for the N³LO corrections $r(n)$ to the anomalous-dimension (AD) function of Eq. (10).

We fix them using the [1/1] Padé resummation procedure of the coefficients of the AD function (for the results, see Table 3, where the expressions which

come from [0/2] Padé estimates are also presented). It should be mentioned that the values for $p(n)$ and $q(n)$ are calculated from the numbers given in Table 1.

Table 2. The values for NLO, NNLO, N³LO QCD contributions to the coefficient functions, used in our fits, and the results of N³LO Padé estimates

n	$C_{F_3}^{(1)}(n)$	$C_{F_3}^{(2)}(n)$	$C_{F_3}^{(2)}(n) _{\text{int}}$	$C_{F_3}^{(3)}(n) _{\text{int}}$	$C_{F_3}^{(3)}(n) _{[1/1]}$	$C_{F_3}^{(3)}(n) _{[0/2]}$
1	-4	-52	-52	-644.3464	-676	480
2	-1.778	-47.472	(-46.4295)	(-1127.454)	-1267.643	174.4079
3	1.667	-12.715	-12.715	-1013.171	97.00418	-47.01328
4	4.867	37.117	(37.0076)	(-410.6652)	283.0851	246.0090
5	7.748	95.4086	95.4086	584.9453	1174.835	1013.328
6	10.351	158.2912	(158.4032)	(1893.575)	2420.569	2167.903
7	12.722	223.8978	223.8978	3450.468	3940.284	3637.790
8	14.900	290.8840	(290.8421)	(5205.389)	5678.657	5360.371
9	16.915	358.5874	358.5874	7120.985	7601.721	7291.305
10	18.791	426.4422	(426.5512)	(9170.207)	9677.391	9391.308
11	20.544	494.1881	494.1881	11332.82	11885.25	11633.28
12	22.201	561.5591	(561.2668)	(13590.97)	14204.22	13991.80
13	23.762	628.4539	628.4539	15923.91	16620.99	16449.68

Table 3. The values for NLO and NNLO QCD contributions to the expanded anomalous dimension terms used in our fits and the N³LO Padé estimates

n	$p(n)$	$q(n)$	$r(n) _{[1/1]}$	$r(n) _{[0/2]}$
1	0	0	0	0
2	1.6462	4.8121	14.0666	11.3822
3	1.9402	5.5018	15.6011	14.0456
4	2.0504	5.8327	16.5919	15.2986
5	2.1149	6.2836	18.6691	17.1187
6	2.1650	6.7445	21.0110	19.0560
7	2.2098	7.1671	23.2447	20.8847
8	2.2525	7.6013	25.6518	22.8152
9	2.2939	8.0164	28.0151	24.7073
10	2.3344	8.4353	30.4804	26.6614
11	2.3741	8.8146	32.7261	28.4720
12	2.4131	9.1855	34.9647	30.2794
13	2.4512	9.5620	37.3002	32.1491

Several comments should be made concerning the comparison of the Padé estimates technique of the N³LO corrections $C_{F_3}^{(3)}(n)$ with more definite to our point of view, results of application of the interpolation procedure (see Table 2). One can see that the agreement of [1/1] Padé estimates with the N³LO coefficients

is good in the case of the Gross–Llewellyn-Smith sum rule (this fact was already known from the estimates of Ref. 47, which are close to the results of the scheme-invariant approach of Ref. 48). In the case of $n = 2$ and $n \geq 6$ moments the numbers of columns 5 and 6 of Table 2 are also in satisfactory agreement. Indeed, one should keep in mind that the difference between the numbers presented in columns 5 and 6 of Table 2 should be divided by the factor $(4)^3$, which comes from our definition of the expansion parameter $A_s = \alpha_s/(4\pi)$. Note that, starting from $n \geq 6$, the results of the application of [0/2] Padé approximants, which in accordance with the analysis of Ref. 49 reduce scale-dependence uncertainties, are even closer to the estimates which are given by the interpolation procedure (for the comparison of the outcome of approximate N³LO fits to xF_3 data, which are based on [1/1] and [0/2] Padé approximants, see Ref. 5, while the comparison of the applications of [1/1] and [0/2] Padé approximants within the quantum-mechanic model was analysed in Ref. 50). For $n = 3, 4$ the interpolation method gives completely different results. The failure of the application of the Padé estimates approach in these cases might be related to the irregular sign structure of the perturbative series under consideration. A similar problem arises in the case of the analysis of the perturbative series for QED renormalization group functions (for discussions, see Ref. 51).

However, in the case of the perturbative series AD for the expanded anomalous-dimension term, we do not face this problem (see Table 3). In view of the absence of other ways of fixation of N³LO coefficients $r(n)$ (the renormalon-inspired large- β_0 expansion is definitely not working for the anomalous-dimensions functions [52, 53]), we will use in our fits the [1/1] Padé estimates for $r(n)$. Note in advance that the application of [0/2] Padé resummation to $r(n)$ does not influence the outcome of our approximate N³LO fits with α_s defined by its explicit N³LO expression (see Eqs. (14)–(16)). It should be stressed that since in the process of these fits we will use the explicitly calculated coefficient functions of the xF_3 Mellin moments [23], the obtained uncertainties will be more definite than those estimated in our previous work of Ref. 5.

3. RESULTS OF THE FITS WITHOUT TWIST-4 TERMS

In order to perform the concrete fits to xF_3 CCFR'97 data and thus analyse how new theoretical input, described in Sec. 2, affects the results previously obtained in Ref. 5, we apply the same theoretical method, based on reconstruction of xF_3 from its Mellin moments using the Jacobi polynomial expansion [8–12]:

$$\begin{aligned} xF_3^{N_{\max}}(x, Q^2) &= \\ &= w(\alpha, \beta)(x) \sum_{n=0}^{N_{\max}} \Theta_n^{\alpha, \beta}(x) \sum_{j=0}^n c_j^{(n)}(\alpha, \beta) M_{j+2, xF_3}^{\text{TMC}}(Q^2) + \frac{h(x)}{Q^2}, \quad (18) \end{aligned}$$

where $\Theta_n^{\alpha,\beta}$ are the Jacobi polynomials; $c_j^{(n)}(\alpha, \beta)$ contain α - and β -dependent Euler Γ functions, where α, β are the Jacobi polynomial parameters, fixed by the minimization of the error in the reconstruction of the SF; and $w(\alpha, \beta) = x^\alpha(1-x)^\beta$ is the corresponding weight function with $\alpha = 0.7$ and $\beta = 3$ chosen following the detailed analysis of Ref.5. The contributions of the dynamical twist-4 terms are modelled by the Q^2 -independent function $h(x)$. The kinematical power corrections, namely, the target mass contributions, are included in the reconstruction formula of Eq.(18) up to the order of $O(M_{\text{nucl}}^2/Q^2)$ terms:

$$M_{n,xF_3}^{\text{TMC}}(Q^2) = M_n^{F_3}(Q^2) + \frac{n(n+1)}{n+2} \frac{M_{\text{nucl}}^2}{Q^2} M_{n+2}^{F_3}(Q^2). \quad (19)$$

Using Eqs. (18), (19), one can conclude that choosing $N_{\text{max}} = 6$, as was done in the case of NNLO fits of Refs.3–5, we are taking into account $2 \leq n \leq 10$ Mellin moments in Eq. (18). As was emphasized above, definite information on the NNLO QCD corrections to the renormalization-group functions of $2 \leq n \leq 13$ moments of xF_3 is now available. In view of this we can now increase the number of N_{max} from $N_{\text{max}} = 6$ to $N_{\text{max}} = 9$ and analyze the changes in the results of the NNLO fits of Ref.5 due to application of additional theoretical information.

We are starting our studies from the case when twist-4 contributions are switched off (namely $h(x) = 0$). In Table 4 we present the dependence of the extracted values of $\Lambda_{\overline{MS}}^{(4)}$ from the variations of N_{max} and of the initial scale Q_0^2 . Looking carefully at Table 4, one can clearly see that the results of the NLO fits are rather stable under the changes of Q_0^2 . Moreover, they are in agreement with the ones presented in Table 3 of Ref.5. However, for $N_{\text{max}} = 10$, the values of χ^2 are larger than for the case of $N_{\text{max}} = 9$. Moreover, we checked that for $Q_0^2 = 20 \text{ GeV}^2$ and $N_{\text{max}} = 11$, despite the fact that the corresponding value $\Lambda_{\overline{MS}}^{(4)} = 334 \pm 37 \text{ MeV}$ is comparable with the one obtained in the case of choosing $N_{\text{max}} = 10$ (see Table 4), χ^2 continues to increase (we got $\chi^2 = 88.9/86$). Therefore, it might be reasonable to stop at $N_{\text{max}} = 9$ and thus take into account in Eq. (18) 13 moments only.

At $N_{\text{max}} = 6$, the new NNLO results agree with the findings of Ref.5. They demonstrate the same dependence of $\Lambda_{\overline{MS}}^{(4)}$ on Q_0^2 . Notice that it has the stability plateau starting from $Q_0^2 = 20 \text{ GeV}^2$ only. However, there is the important difference between the results of the NNLO fits of the current work and the ones of Ref.5. Indeed, at the NNLO, Table 4 demonstrates the widening of the stability plateau for $\Lambda_{\overline{MS}}^{(4)}$ to lower Q_0^2 values for $7 \leq N_{\text{max}} \leq 9$ and the minimization of the χ^2 value at $N_{\text{max}} = 9$. This welcome feature is showing us the importance of changing the approximate expressions for $\gamma_{\text{NS}}^{(2)}(n)$ from the model $\gamma_{F_3}^{(2)}(n) \approx \gamma_{\text{NS},F_2}^{(2)}(n)$ used in [5] to the new one, which is based on the *exact numbers* for $\gamma_{F_3}^{(2)}(n)$, calculated in [23] *plus* application of the fine-tuning

Table 4. The Q_0^2 and N_{\max} dependence of $\Lambda_{\overline{MS}}^{(4)}$ (MeV). The values of χ^2 are presented in parenthesis

N_{\max}	Q_0^2 , GeV ²	5	8	10	20	50	100
10	LO	266 ± 35 (113.2)	265 ± 36 (113.2)	265 ± 38 (113.2)	264 ± 35 (113.1)	264 ± 36 (112.9)	263 ± 36 (112.6)
6	NLO	341 ± 37 (85.4)	341 ± 37 (85.7)	340 ± 37 (85.7)	340 ± 36 (85.7)	339 ± 37 (85.4)	338 ± 37 (85.1)
7	NLO	342 ± 38 (87.1)	341 ± 38 (87.3)	341 ± 37 (87.4)	340 ± 37 (87.4)	339 ± 37 (87.2)	338 ± 37 (86.9)
8	NLO	346 ± 38 (86.0)	344 ± 38 (86.4)	344 ± 38 (86.5)	343 ± 37 (86.5)	341 ± 38 (86.2)	341 ± 38 (85.9)
9	NLO	349 ± 42 (84.2)	347 ± 37 (84.8)	347 ± 37 (85.0)	345 ± 38 (85.1)	344 ± 37 (84.8)	343 ± 38 (84.5)
10	NLO	341 ± 35 (87.1)	340 ± 33 (87.4)	339 ± 34 (87.5)	338 ± 40 (87.6)	337 ± 37 (87.5)	336 ± 35 (87.3)
6	NNLO	297 ± 30 (77.9)	314 ± 34 (76.3)	320 ± 34 (76.2)	327 ± 36 (76.9)	327 ± 35 (78.5)	326 ± 35 (79.5)
7	NNLO	326 ± 34 (75.9)	327 ± 35 (76.7)	327 ± 35 (77.1)	326 ± 36 (78.1)	327 ± 36 (78.8)	328 ± 35 (78.7)
8	NNLO	334 ± 35 (74.3)	334 ± 35 (75.7)	333 ± 35 (76.2)	331 ± 35 (77.4)	328 ± 35 (78.3)	328 ± 35 (78.5)
9	NNLO	330 ± 33 (72.4)	332 ± 35 (73.6)	333 ± 34 (74.7)	331 ± 37 (75.8)	330 ± 35 (76.7)	329 ± 35 (77.8)
6	N ³ LO	303 ± 29 (76.4)	317 ± 31 (75.6)	321 ± 32 (75.7)	325 ± 33 (76.6)	325 ± 33 (78.0)	324 ± 33 (78.7)
7	N ³ LO	328 ± 32 (76.2)	326 ± 33 (77.0)	325 ± 33 (77.3)	322 ± 33 (78.2)	324 ± 33 (78.5)	324 ± 33 (78.2)
8	N ³ LO	334 ± 33 (74.8)	329 ± 33 (76.2)	327 ± 34 (76.6)	324 ± 34 (77.4)	323 ± 34 (77.3)	324 ± 34 (77.2)
9	N ³ LO	330 ± 31 (73.3)	329 ± 34 (74.6)	329 ± 32 (75.7)	325 ± 33 (76.4)	325 ± 32 (76.7)	325 ± 33 (76.8)

procedure, which in the case of $N_{\max} = 6$ gives $\gamma_{F_3}^{(2)}(6) = 1247.4222 \pm 2.1357$; for $N_{\max} = 7$ gives $\gamma_{F_3}^{(2)}(6) = 1248.1219 \pm 1.0359$, $\gamma_{F_3}^{(2)}(8) = 1420.1729 \pm 4.0854$; for $N_{\max} = 8$ gives $\gamma_{F_3}^{(2)}(6) = 1248.5610 \pm 1.2951$, $\gamma_{F_3}^{(2)}(8) = 1419.3301 \pm 1.5112$, $\gamma_{F_3}^{(2)}(10) = 1561.4299 \pm 1.4074$; and for $N_{\max} = 9$ gives $\gamma_{F_3}^{(2)}(6) = 1247.7852 \pm 0.5091$, $\gamma_{F_3}^{(2)}(8) = 1420.2215 \pm 0.3337$, $\gamma_{F_3}^{(2)}(10) = 1560.8461 \pm 0.2292$. Within the quoted error bars, these fine-tuned numbers agree with the estimates obtained by smooth polynomial interpolation and presented in the last column of Table 1. The agreement improves with increasing of N_{\max} . In the case of $N_{\max} = 9$, the difference is in the 4th significant digit.

However, the improved Q_0^2 -independent NNLO values of $\Lambda_{\overline{MS}}^{(4)}$ do not differ significantly from the results of Ref. 5 (the difference of over 4–5 MeV is about 7 times smaller than the existing statistical error). A similar feature reveals itself in the process of the N³LO fits, which are based in part on application of the *exact numbers* for the α_s^3 corrections to the coefficient functions of odd Mellin moments, calculated in [23], and were performed using the N³LO approximation of α_s . It should be stressed that the inclusion in the fits of these numbers at $N_{\max} = 6$ does not lead to a detectable difference of the new results from the ones obtained in [5] with the help of the Padé approximation method. The essential advantage of the new considerations is that we are able to reach $N_{\max} = 9$ and observe perfect stability of both NNLO and new N³LO values for $\Lambda_{\overline{MS}}^{(4)}$ to the variation of Q_0^2 after slight modification of $\gamma_{F_3}^{(2)}(6)$, $\gamma_{F_3}^{(2)}(8)$, and $\gamma_{F_3}^{(2)}(10)$ (which arise from the application of fine-tuning procedure at the N³LO), and can determine from these numbers the Padé approximations for $r(n)|_{[1/1]}$ at $n = 6, 8, 10$. It should be mentioned that the obtained estimates for the fitted three terms of $\gamma_{F_3}^{(2)}(n)$ are in agreement with the estimates presented above at the level of four significant digits. Note also that if we use in the fits [0/2] Padé approximants for modelling the N³LO correction $r(n)$, we get the values of $\Lambda_{\overline{MS}}^{(4)}$, which are rather close to those obtained in the case of application of [1/1] Padé approximants.

Comparing now the results of the NNLO and approximate N³LO fits, we conclude that for $7 \leq N_{\max} \leq 9$ the difference between the obtained values of $\Lambda_{\overline{MS}}^{(4)}$ is rather small and almost disappears for $Q_0^2 = 5 \text{ GeV}^2$. Thus, we can make the conclusion that we observe the minimization of theoretical uncertainties and, probably, the saturation of the predictive power of the corresponding perturbative series at the 4-loop level. A similar feature was discovered in the process of calculations of the perturbative corrections to the correlator of scalar quark currents in the large- f approximation [54]. Therefore, we think that the perturbation-theory approximants for xF_3 moments can be safely truncated at one more step beyond the NNLO. Higher-order calculations might manifest the signal for asymptotic divergence of the related perturbative QCD predictions and, as a result, the increase of the value of χ^2 .

Another consequence of our new improved analysis corresponds to the determination of the Q_0^2 dependence of the parameters A , b , c , and γ . It is presented in Table 5 and is compared with the previous extraction of their Q_0^2 dependence given in Ref. 4. The LO and NLO numbers are the same, while at the NNLO the new results in bold type, which correspond to $N_{\max} = 9$, are compared with the previous NNLO ones [4], obtained at $N_{\max} = 6$ using the calculations of $\gamma_{\text{NS}, F_2}^{(2)}(n)$ terms [19, 20] available at this time. One can see a noticeable decrease in χ^2 at the NNLO. In the LO, the obtained Q_0^2 dependence of c is in agreement with the shape of variation of this parameter predicted in Ref. 55 and confirmed recently in Ref. 56.

Table 5. The determined values of the parameters A, b, c, γ of the model for xF_3 and their comparison with the values obtained in [4]. The new ones, related to the NNLO, are in bold type

Order/ N_{\max}	Q_0^2 , GeV ²	A	b	c	γ	χ^2/nop
LO/9	5	5.13 ± 0.21	0.72 ± 0.01	3.87 ± 0.06	1.42 ± 0.20	113.2/86
	10	5.07 ± 0.22	0.70 ± 0.01	3.97 ± 0.08	1.16 ± 0.25	113.2/86
	20	4.98 ± 0.47	0.68 ± 0.03	4.05 ± 0.10	0.96 ± 0.41	113.1/86
	100	4.73 ± 0.36	0.64 ± 0.02	4.19 ± 0.09	0.62 ± 0.30	112.6/86
NLO/9	5	4.05 ± 0.20	0.65 ± 0.02	3.71 ± 0.06	1.93 ± 0.16	87.1/86
	10	4.48 ± 0.21	0.66 ± 0.02	3.85 ± 0.05	1.32 ± 0.15	87.5/86
	20	4.48 ± 0.21	0.65 ± 0.01	3.96 ± 0.07	0.95 ± 0.15	87.6/86
	100	4.73 ± 0.38	0.62 ± 0.02	4.12 ± 0.12	0.46 ± 0.34	87.3/86
NNLO/6 NNLO/9 NNLO/6 NNLO/9 NNLO/6 NNLO/9 NNLO/6 NNLO/9	5	4.25 ± 0.38	0.66 ± 0.03	3.56 ± 0.07	1.33 ± 0.33	78.4/86
		3.73 ± 0.68	0.63 ± 0.05	3.52 ± 0.08	1.69 ± 0.68	72.4/86
	10	4.50 ± 0.36	0.65 ± 0.03	3.73 ± 0.07	1.05 ± 0.31	76.3/86
		4.21 ± 0.35	0.63 ± 0.03	3.73 ± 0.07	1.22 ± 0.31	74.2/86
	20	4.70 ± 0.34	0.65 ± 0.03	3.88 ± 0.08	0.80 ± 0.30	77.0/86
		4.49 ± 0.25	0.63 ± 0.02	3.89 ± 0.06	0.93 ± 0.20	75.8/86
	100	4.91 ± 0.28	0.63 ± 0.02	4.11 ± 0.10	0.53 ± 0.27	80.0/86
		4.74 ± 0.32	0.61 ± 0.02	4.14 ± 0.09	0.46 ± 0.27	77.8/86
N ³ LO/9 N ³ LO/9 N ³ LO/9 N ³ LO/9	5	4.16 ± 0.28	0.65 ± 0.02	3.31 ± 0.09	0.91 ± 0.21	73.3/86
	10	4.49 ± 0.41	0.65 ± 0.03	3.61 ± 0.08	0.81 ± 0.32	75.1/86
	20	4.64 ± 0.72	0.64 ± 0.05	3.83 ± 0.15	0.73 ± 0.60	76.4/86
	100	4.77 ± 0.30	0.61 ± 0.02	4.15 ± 0.09	0.47 ± 0.26	77.6/86

Even more, it is interesting to study our NNLO results for the parameter $b(Q_0^2)$. First, it is almost Q_0^2 -independent within statistical errors. This fact is in agreement with theoretical demonstration of its Q_0^2 independence, presented in [57] using DGLAP equation. Another result was obtained recently in [58] in all orders of 1-loop expression for α_s , using in part the approach, developed in [59]. It should be stressed that the estimate $\omega^- = 0.4$ in the expression $F_{\text{NS}} = (1/x)^{\omega^-} (Q^2/\mu^2)^{\omega^-/2}$, obtained in Ref. 58 for $\mu \approx 5.5$ GeV, $\Lambda_{\text{QCD}} = 0.1$, and $f = 3$ is in good numbers for $1 - b$, especially in the region $Q^2 > \mu^2 = 30$ GeV², which is not considerably affected by the transformation from $\Lambda^{(3)} \approx 0.1$ GeV, used in Ref. 58, to $\Lambda_{\overline{MS}}^{(3)} \approx 0.4$ GeV, as advocated by us.

4. INCORPORATION OF THE TWIST-4 TERMS

4.1. Infrared Renormalon Model Parameterization. The next stage in modification of QCD theoretical approximations is the inclusion of the higher-twist terms in the expression for the structure functions. At the first stage we will

rely on the prediction of the IRR approach [29] and model the twist-4 contribution to $h(x)$ in Eq. (18) as

$$\frac{h(x)}{Q^2} = w(\alpha, \beta) \sum_{n=0}^{N_{\max}} \Theta_n^{\alpha, \beta}(x) \sum_{j=0}^n c_j^{(n)}(\alpha, \beta) M_{j+2, xF_3}^{\text{IRR}}(Q^2), \quad (20)$$

where

$$M_{n, xF_3}^{\text{IRR}}(Q^2) = \tilde{C}(n) M_n^{F_3}(Q^2) \frac{A_2'}{Q^2}$$

with $\tilde{C}(n) = -n - 4 + 2/(n+1) + 4/(n+2) + 4S_1(n)$. (21)

The results of the new improved fits to CCFR'97 data for xF_3 with the twist-4 term taken into account through Eq. (21) are presented in Table 6.

Looking carefully at Table 6 we arrive at the following new conclusions:

- The χ^2 value decreases from LO up to NNLO and at N³LO level it almost coincides with the one obtained at the NNLO. Moreover, χ^2 decreases with the increasing of N_{\max} and distinguishes the fits with $N_{\max} = 9$. This is a welcome feature of including in the fitting procedure more detailed information on the perturbative theory contributions to both coefficient functions and anomalous dimensions of xF_3 moments, and in particular explicitly-calculated three-loop coefficients $\gamma_{F_3}^{(2)}(n)$ at $n = 3, 5, 7, 9, 11, 13$ [23], supplemented by us with application of the interpolation procedure for even n plus fine-tuning of the terms $\gamma_{F_3}^{(2)}(6)$, $\gamma_{F_3}^{(2)}(8)$, and $\gamma_{F_3}^{(2)}(10)$.

- At the N³LO, χ^2 is smaller than the one obtained in the process of pure Padé-motivated fits of Ref. 5. This feature is related to the fact that the explicit expressions for N³LO corrections for odd xF_3 moments [23] are now taken into account.

- For $N_{\max} = 9$, the values of $\Lambda_{\overline{MS}}^{(4)}$ and the IRR model free parameter A_2' are rather stable to variation of Q_0^2 not only at the LO, NLO, but at the NNLO and N³LO as well. The last property gives favour to our new results in comparison with the ones obtained in Ref. 5 in the case of $N_{\max} = 6$ and $Q_0^2 = 20 \text{ GeV}^2$, taking into account a more approximate model for $\gamma_{F_3}^{(2)}(n)$ and Padé approximations for $C_{F_3}^{(3)}(n)$ at $n \leq 10$.

- At the scale $Q_0^2 = 20 \text{ GeV}^2$, the obviously visible difference with the findings of Ref. 5 is related to the switch from the Padé approximant estimates of N³LO contributions to coefficient functions to the expressions for $C_{F_3}^{(3)}|_{\text{int}}$, presented in Table 2, and obtained from the calculations of $C_{F_3}^{(3)}(n)$ at $n = 1$ [27] and $n = 3, 5, 7, 9, 11, 13$ [23]. The positive outcome of this change is the shift of $\Lambda_{\overline{MS}}^{(4)}$ from $340 \pm 37 \text{ MeV}$ to the values, given in Table 6 (which are less different from the results of the NNLO fits) and the minimization of the value of χ^2 .

Table 6. The results of the fits to the CCFR'97 xF_3 data with HT terms modelled through the IRR model. A_2' is the additional parameter of the fit. The cases of different Q_0^2 and N_{\max} are considered

Order/ N_{\max}	$Q_0^2 =$	5 GeV ²	20 GeV ²	100 GeV ²
LO/6	$\Lambda_{\overline{MS}}^{(4)}$	433 ± 54	431 ± 36	429 ± 35
	χ^2/nep	81.2/86	81.2/86	80.6/86
	A_2'	-0.331 ± 0.057	-0.330 ± 0.059	-0.328 ± 0.058
LO/9	$\Lambda_{\overline{MS}}^{(4)}$	447 ± 54	443 ± 54	439 ± 56
	χ^2/nep	79.8/86	80.1/86	79.6/86
	A_2'	-0.340 ± 0.059	-0.337 ± 0.059	-0.335 ± 0.059
NLO/6	$\Lambda_{\overline{MS}}^{(4)}$	370 ± 38	369 ± 41	367 ± 38
	χ^2/nep	80.2/86	80.4/86	79.9/86
	A_2'	-0.121 ± 0.052	-0.121 ± 0.053	-0.120 ± 0.052
NLO/9	$\Lambda_{\overline{MS}}^{(4)}$	379 ± 41	376 ± 39	374 ± 42
	χ^2/nep	78.6/86	79.5/86	79.0/86
	A_2'	-0.125 ± 0.053	-0.125 ± 0.053	-0.124 ± 0.053
NNLO/6	$\Lambda_{\overline{MS}}^{(4)}$	297 ± 30	328 ± 36	328 ± 35
	χ^2/nep	77.9/86	76.8/86	79.5/86
	A_2'	-0.007 ± 0.051	-0.017 ± 0.051	-0.015 ± 0.051
NNLO/7	$\Lambda_{\overline{MS}}^{(4)}$	327 ± 34	327 ± 35	328 ± 36
	χ^2/nep	75.8/86	78.1/86	78.6/86
	A_2'	-0.011 ± 0.051	-0.013 ± 0.051	-0.015 ± 0.051
NNLO/8	$\Lambda_{\overline{MS}}^{(4)}$	335 ± 37	330 ± 36	329 ± 36
	χ^2/nep	73.8/86	77.0/86	77.5/86
	A_2'	-0.012 ± 0.051	-0.013 ± 0.051	-0.015 ± 0.051
NNLO/9	$\Lambda_{\overline{MS}}^{(4)}$	331 ± 33	332 ± 35	331 ± 35
	χ^2/nep	73.1/86	75.7/86	76.9/86
	A_2'	-0.013 ± 0.051	-0.015 ± 0.051	-0.016 ± 0.051
N ³ LO/6	$\Lambda_{\overline{MS}}^{(4)}$	305 ± 29	327 ± 34	326 ± 34
	χ^2/nep	76.0/86	76.2/86	78.5/86
	A_2'	0.036 ± 0.051	0.033 ± 0.052	0.029 ± 0.052
N ³ LO/7	$\Lambda_{\overline{MS}}^{(4)}$	331 ± 33	325 ± 34	326 ± 34
	χ^2/nep	75.6/86	77.7/86	77.8/86
	A_2'	0.040 ± 0.052	0.036 ± 0.052	0.035 ± 0.052
N ³ LO/8	$\Lambda_{\overline{MS}}^{(4)}$	337 ± 34	326 ± 34	326 ± 34
	χ^2/nep	74.1/86	76.9/86	76.7/86
	A_2'	0.040 ± 0.052	0.036 ± 0.052	0.035 ± 0.052
N ³ LO/9	$\Lambda_{\overline{MS}}^{(4)}$	333 ± 34	328 ± 33	328 ± 38
	χ^2/nep	73.8/86	75.9/86	76.4/86
	A_2'	0.038 ± 0.052	0.035 ± 0.052	0.034 ± 0.052

• The LO and NLO fits seem to support the IRR model for the twist-4 terms by the foundation of negative values of A'_2 , which are different from zero within the presented error bars and are in agreement with the results of the previous similar fits of Refs. 3, 5 and with the one obtained in Ref. 38 using the NLO DGLAP analysis of the same set of CCFR'97 data.

• At the NNLO, the central value of A'_2 is also negative but has large error bars. Moreover, the inclusion of the N³LO corrections clearly demonstrates the effective minimization of the free parameter of the IRR model, which becomes positive but has statistical uncertainties twice as large as the central value. Thus, we may conclude that at this level, the interplay between high-order perturbative corrections and the model for twist-4 contributions, discussed from various points of view in Refs. 60–62, is manifests itself.

4.2. IRR Approach and Naive Non-Abelianization. Perturbative expansion of the IRR model is usually understood within the framework of the large- β_0 expansion, where β_0 is the first coefficient of the QCD β function. The approximations for coefficient functions (but not anomalous dimensions) obtained within this model can be compared with the explicit expression for the quantities under consideration, calculated in the \overline{MS} scheme. As a rule, the qualitative success of the estimating power of the large- β_0 expansion is rather satisfactory (see, e. g., [32,54]). Let us study the application of this approach to the coefficient functions of odd Mellin moments of $x F_3$ used in our work.

They can be presented in the following numerical form (see Refs. 23, 27):

$$\begin{aligned}
C_{F_3}^{(1)} &= 1 - 4A_s + A_s^2(-73.333 + 5.333f) + \\
&\quad + A_s^3(-2652.154 + 513.310f - 11.358f^2), \\
C_{F_3}^{(3)} &= 1 + 1.667A_s + A_s^2(14.254 - 6.742f) + \\
&\quad + A_s^3(-839.764 - 45.099f + 1.748f^2), \\
C_{F_3}^{(5)} &= 1 + 7.748A_s + A_s^2(173.001 - 19.398f) + \\
&\quad + A_s^3(4341.081 - 961.276f + 22.241f^2), \\
C_{F_3}^{(7)} &= 1 + 12.722A_s + A_s^2(345.991 - 30.523f) + \\
&\quad + A_s^3(11119.001 - 1960.237f + 43.104f^2), \\
C_{F_3}^{(9)} &= 1 + 16.915A_s + A_s^2(520.006 - 40.355f) + \\
&\quad + A_s^3(18771.996 - 2975.924f + 63.171f^2), \\
C_{F_3}^{(11)} &= 1 + 20.548A_s + A_s^2(690.872 - 49.171f) + \\
&\quad + A_s^3(26941.480 - 3984.412f + 82.246f^2), \\
C_{F_3}^{(13)} &= 1 + 23.762A_s + A_s^2(857.178 - 57.181f) + \\
&\quad + A_s^3(35426.829 - 4976.081f + 100.351f^2).
\end{aligned} \tag{22}$$

Note that for the reasons discussed below, the order $O(A_s^3)$ -order corrections to Eq. (22) are presented without typical structures (wt_s) proportional to $d^{abc}d^{abc}$ terms.

The procedure of large- β_0 expansion is formulated in our notations in the following way: one should extract from the explicit expressions for perturbative coefficients, calculated in the \overline{MS} -scheme, the leading terms in the number of flavours f and then make the substitution $f \rightarrow -6\tilde{\beta}_0$, where $\tilde{\beta}_0 = \beta_0/4$. This approximation is known in the literature as the «naive non-Abelianization» (NNA) procedure [63]. Note that it does not simulate $d^{abc}d^{abc}$ terms. Using this pattern, we present below the coefficient functions of Eq. (22) in the NNA form:

$$\begin{aligned}
 C_{F_3}^{(1)} &= 1 - 4A_s + A_s^2(-6 \times 5.333\tilde{\beta}_0) + A_s^3(-36 \times 11.358\tilde{\beta}_0^2), \\
 C_{F_3}^{(3)} &= 1 + 1.667A_s + A_s^2(6 \times 6.742\tilde{\beta}_0) + A_s^3(36 \times 1.748\tilde{\beta}_0^2), \\
 C_{F_3}^{(5)} &= 1 + 7.748A_s + A_s^2(6 \times 19.398\tilde{\beta}_0) + A_s^3(36 \times 22.241\tilde{\beta}_0^2), \\
 C_{F_3}^{(7)} &= 1 + 12.722A_s + A_s^2(6 \times 30.523\tilde{\beta}_0) + A_s^3(36 \times 43.104\tilde{\beta}_0^2), \quad (23) \\
 C_{F_3}^{(9)} &= 1 + 16.915A_s + A_s^2(6 \times 40.355\tilde{\beta}_0) + A_s^3(36 \times 63.171\tilde{\beta}_0^2), \\
 C_{F_3}^{(11)} &= 1 + 20.548A_s + A_s^2(6 \times 49.171\tilde{\beta}_0) + A_s^3(36 \times 82.246\tilde{\beta}_0^2), \\
 C_{F_3}^{(13)} &= 1 + 23.762A_s + A_s^2(6 \times 57.181\tilde{\beta}_0) + A_s^3(36 \times 100.351\tilde{\beta}_0^2).
 \end{aligned}$$

The obtained NNLO and N³LO corrections should be compared with the corresponding ones of Eqs. (24). The f dependence of the ratios $R_{F_3, \text{NNA}}^{(2)}(n) = C_{F_3}^{(2)}(n)_{\text{NNA}}/C_{F_3}^{(2)}(n)$ and $R_{F_3, \text{NNA}}^{(3)}(n) = C_{F_3}^{(3)}(n)_{\text{NNA}}/C_{F_3}^{(3)}(n)|_{wt_s}$, which follow from the comparison of the related expressions of Eqs. (22), (23), is presented in Table 7 and Table 8, where the f dependence of the ratio $R_{F_3}^{(3)}(n)|_{[\text{Pade}]} = C_{F_3}^{(3)}(n)|_{[1/1]}/C_{F_3}^{(3)}(n)|_{wt_s}$ is also given in round brackets.

One can see that the NNA approach is working reasonably well in the case of the Gross–Llewellyn–Smith sum rule ($n = 1$ moment). This fact was already observed in the review of Ref. 32. It also gives satisfactory estimates both at the NNLO and N³LO in the case of odd values of n with $n \geq 7$, but does not work for $n = 3$ (where even the wrong sign is obtained) and for $n = 5$, where at the N³LO the subleading in f (and thus β_0) term is larger than the leading β_0^2 contribution. Notice that in the case of even NS moments of F_2 the situation was the same: the NNA approximation was predicting the correct sign starting from the $n = 4$ moment and was giving qualitatively good estimates in the cases of $n = 6, 8$ moments [34]. Armed with this new information about explicit behaviour of the NS moments for F_2 with $n = 10$ [20] and $n = 12, 14$ [23], we extend the considerations of Ref. 34 to the case of higher moments, omitting $f \sum_{f=1}^f e_f$ contribution to the order $O(A_s^3)$ -order corrections of the NS moments

Table 7. The f dependence of the ratios $R_{F_3, \text{NNA}}^{(2)}(n)$

n	$f = 3$	$f = 4$	$f = 5$
1	1.25	1.28	1.31
3	-15.24	-6.63	-3.98
5	2.34	2.61	3.07
7	1.43	1.42	1.41
9	1.36	1.41	1.46
11	1.22	1.24	1.27
13	1.13	1.14	1.15

Table 8. The f dependence of the ratios $R_{F_3, \text{NNA}}^{(3)}(n)$ and $R_{F_3}^{(3)}(n)|_{[\text{Pade}]}$ (in round brackets)

n	$f = 3$	$f = 4$	$f = 5$
1	1.61 (0.68)	2.01 (0.87)	2.99 (1.48)
3	-0.32 (-0.002)	-0.26 (-0.1)	-0.21 (-0.22)
5	2.46 (1.03)	4.15 (1.38)	41.32 (8.22)
7	1.4 (0.90)	1.7 (0.99)	2.4 (1.22)
9	1.1 (0.90)	1.25 (0.96)	1.56 (1.09)
11	0.95 (0.91)	1.04 (0.96)	1.20 (1.06)
13	0.85 (0.92)	0.95 (0.97)	1.02 (1.05)

of F_2 . Taking into account this approximation, we present the explicit expressions for the coefficient functions of the NS moments of F_2 in the following numerical form:

$$\begin{aligned}
C_{F_2, \text{NS}}^{(2)} &= 1 + 0.444A_s + A_s^2(17.694 - 5.333f) + \\
&\quad + A_s^3(442.741 - 165.197f + 6.030f^2), \\
C_{F_2, \text{NS}}^{(4)} &= 1 + 6.607A_s + A_s^2(141.344 - 16.988f) + \\
&\quad + A_s^3(4169.268 - 901.235f + 23.355f^2), \\
C_{F_2, \text{NS}}^{(6)} &= 1 + 11.177A_s + A_s^2(302.399 - 28.013f) + \\
&\quad + A_s^3(10069.631 - 1816.323f + 42.663f^2), \\
C_{F_2, \text{NS}}^{(8)} &= 1 + 15.530A_s + A_s^2(470.807 - 37.925f) + \\
&\quad + A_s^3(17162.372 - 2787.298f + 61.9118f^2), \\
C_{F_2, \text{NS}}^{(10)} &= 1 + 19.301A_s + A_s^2(639.211 - 46.861f) + \\
&\quad + A_s^3(24953.135 - 3770.102f + 80.5201f^2),
\end{aligned} \tag{24}$$

$$\begin{aligned}
 C_{F_2,NS}^{(12)} &= 1 + 22.628A_s + A_s^2(804.585 - 54.994f) + \\
 &\quad + A_s^3(33171.455 - 4746.441f + 98.348f^2), \\
 C_{F_2,NS}^{(14)} &= 1 + 25.611A_s + A_s^2(965.813 - 62.465f) + \\
 &\quad + A_s^3(41657.116 - 5708.216f + 115.392f^2).
 \end{aligned}$$

The NNA versions of the expressions from Eq. (24) read:

$$\begin{aligned}
 C_{F_2,NS}^{(2)} &= 1 + 0.444A_s + A_s^2(6 \times 5.333\tilde{\beta}_0) + A_s^3(36 \times 6.030\tilde{\beta}_0^2), \\
 C_{F_2,NS}^{(4)} &= 1 + 6.607A_s + A_s^2(6 \times 16.988\tilde{\beta}_0) + A_s^3(36 \times 23.355\tilde{\beta}_0^2), \\
 C_{F_2,NS}^{(6)} &= 1 + 11.177A_s + A_s^2(6 \times 28.013\tilde{\beta}_0) + A_s^3(36 \times 42.663\tilde{\beta}_0^2), \\
 C_{F_2,NS}^{(8)} &= 1 + 15.530A_s + A_s^2(6 \times 37.925\tilde{\beta}_0) + A_s^3(36 \times 61.9118\tilde{\beta}_0^2), \quad (25) \\
 C_{F_2,NS}^{(10)} &= 1 + 19.301A_s + A_s^2(6 \times 46.861\tilde{\beta}_0) + A_s^3(36 \times 80.5201\tilde{\beta}_0^2), \\
 C_{F_2,NS}^{(12)} &= 1 + 22.628A_s + A_s^2(6 \times 54.994\tilde{\beta}_0) + A_s^3(36 \times 98.348\tilde{\beta}_0^2), \\
 C_{F_2,NS}^{(14)} &= 1 + 25.611A_s + A_s^2(6 \times 62.465\tilde{\beta}_0) + A_s^3(36 \times 115.392\tilde{\beta}_0^2).
 \end{aligned}$$

The numerical values of the ratios of the coefficients of Eqs. (24), (25), namely

$$R_{F_2,NNA}^{(2)}(n) = C_{F_2,NS}^{(2)}(n)_{NNA} / C_{F_2,NS}^{(2)}(n)$$

and

$$R_{F_2,NNA}^{(3)}(n) = C_{F_2,NS}^{(3)}(n)_{NNA} / C_{F_2,NS}^{(3)}(n)|_{wts}$$

are given in Tables 9, 10. In Table 10 $R_{F_2,NNA}^{(3)}(n)$ is compared with

$$R_{F_2}^{(3)}(n)|_{[Pad\acute{e}]} = C_{F_2}^{(3)}(n)|_{[1/1]} / C_{F_2}^{(3)}(n)|_{wts}.$$

Getting support from the related results for $n = 10, 12, 14$ NS moments of F_2 , we can make the conclusion that the findings of Ref. 34 and the new numbers for the moments of xF_3 (see Tables 7, 8) demonstrate that, at the NNLO and N³LO the NNA approximation is working in the NS channel for $n = 1$ and $n \geq 6$, which corresponds to the region of x , closer to the limit $x = 1$. In the cases of low NS moments, the reason for failure of the NNA approximation remains unclear. A similar conclusion can be drawn from the comparison of the [1/1] Padé estimates for $C_{F_3}^{(3)}$ terms with the results of the interpolation procedure (see Table 2 and related discussions after it) and the f dependence of the ratios $R_{F_3,NNA}^{(3)}(n)$ vs $R_{F_3}^{(3)}(n)|_{[Pad\acute{e}]}$ and $R_{F_2,NNA}^{(3)}(n)$ vs $R_{F_2}^{(3)}(n)|_{[Pad\acute{e}]}$ (see Tables 8, 10).

This interesting similarity might be explained by the studies of the large- β_0 limit of the Padé approximant approach [64] and its relation to the BLM

Table 9. The f dependence of the ratios $R_{F_2, \text{NNA}}^{(2)}(n)$

n	$f = 3$	$f = 4$	$f = 5$
2	43.24	-18.17	-3.27
4	2.54	2.89	3.43
6	1.74	1.83	1.98
8	1.43	1.48	1.55
10	1.28	1.29	1.33
12	1.16	1.18	1.19
14	1.08	1.09	1.10

Table 10. The f dependence of the ratios $R_{F_2, \text{NNA}}^{(3)}(n)$ and $R_{F_2}^{(3)}(n)|_{[\text{Padé}]}$

n	$f = 3$	$f = 4$	$f = 5$
2	773.92 (4.56)	-7.75 (-0.24)	-3.41 (-0.22)
4	2.54 (0.73)	3.89 (0.87)	12.51 (1.95)
6	1.55 (0.85)	1.19 (0.93)	2.74 (1.95)
8	1.18 (0.88)	1.38 (0.94)	1.71 (1.07)
10	1.00 (0.90)	1.13 (0.95)	1.31 (1.05)
12	0.90 (0.91)	1.02 (0.96)	1.09 (1.04)
14	0.82 (0.93)	0.87 (0.97)	0.95 (1.04)

approach [65]. Note in these circumstances that, within the large- β_0 limit, the BLM approach was extended to all orders in perturbation theory in [66], while the possibility of incorporation of the subleading terms in the number of flavours f and construction of the NNLO generalization of the BLM approach was first demonstrated in Ref. 67 (for further related analysis see Ref. 68). On the other hand, the qualitative success of application of [1/1] Padé approximation for $n \geq 6$ might be considered as the additional argument in favour of possibility of its application for estimating the N³LO contribution $r(n)$ to the expanded anomalous dimension term Eq. (10).

4.3. The Determination of $\alpha_s(M_Z)$ Values and Their Scale-Dependence Uncertainties. As is known from Refs. 35, 69, it is rather instructive to consider the sensitivity of the results of the perturbative QCD analysis to the variation of renormalization and factorization scales. We will study the question of factorization-renormalization scale dependence within the class of \overline{MS} -like schemes. This means that we will change only the scales without varying the scheme-dependent coefficients of anomalous dimensions and β function.

The arbitrary factorization scale enters in the following equation:

$$A_s(Q^2/\mu_{\overline{MS}}^2) = A_s(Q^2/\mu_F^2) \left[1 + k_1 A_s(Q^2/\mu_F^2) + k_2 A_s^2(Q^2/\mu_F^2) + k_3 A_s^3(Q^2/\mu_F^2) \right], \quad (26)$$

where μ_F^2 is the factorization scale and

$$k_1 = \beta_0 \ln \left(\frac{\mu_{\overline{MS}}^2}{\mu_F^2} \right), \quad k_2 = k_1^2 + \frac{\beta_1}{\beta_0} k_1, \quad k_3 = k_1^3 + \frac{5\beta_1}{2\beta_0} k_1^2 + \frac{\beta_2}{\beta_0} k_1. \quad (27)$$

Let us choose the factorization scale as $\mu_F^2 = \mu_{\overline{MS}}^2 k_F$.

Then we have

$$k_1 = -\beta_0 \ln(k_F). \quad (28)$$

In this case, after application of the renormalization group equation and substitution of Eq. (26) into Eqs. (9), (10) of Sec. 1 we get

$$\exp \left[- \int^{A_s(Q^2/k_F)} \frac{\gamma_{\text{NS}}^{(n)}(x)}{\beta(x)} dx \right] = (A_s(Q^2/k_F))^a \times \overline{AD}(n, A_s(Q^2/k_F)), \quad (29)$$

where $a = \gamma_{\text{NS}}^{(0)}/2\beta_0$ and

$$\begin{aligned} \overline{AD}(n, A_s(Q^2/k_F)) &= 1 + [p(n) + ak_1] A_s(Q^2/k_F) + \\ &+ \left[q(n) + p(n)k_1(a+1) + \frac{\beta_1}{\beta_0} k_1 a + \frac{a(a+1)}{2} k_1^2 \right] A_s^2(Q^2/k_F) + \\ &+ \left[r(n) + q(n)k_1(a+2) + p(n) \left(\frac{\beta_1}{\beta_0} k_1(a+1) + \frac{(a+1)(a+2)}{2} k_1^2 \right) + \right. \\ &\left. + \frac{\beta_2}{\beta_0} k_1 a + \frac{\beta_1}{\beta_0} k_1^2 a \left(\frac{3}{2} + a \right) + \frac{a(a+1)(a+2)}{6} k_1^3 \right] A_s^3(Q^2/k_F). \quad (30) \end{aligned}$$

Now let us consider the factorization-renormalization scale dependence, fixing $k_R = k_F = k$. In this case we should also modify the coefficient function in Eq. (6) as

$$\begin{aligned} C_{F_3}^{(n)} &= 1 + C_{F_3}^{(1)}(n) A_s(Q^2/k) + \left[C_{F_3}^{(2)}(n) - C_{F_3}^{(1)}(n) \beta_0 \ln(k) \right] A_s^2 \left(\frac{Q^2}{k} \right) + \\ &+ \left[C_{F_3}^{(3)}(n) + C_{F_3}^{(1)}(n) (\beta_0^2 \ln^2(k) - \beta_1 \ln(k)) - 2C_{F_3}^{(2)}(n) \beta_0 \ln(k) \right] A_s^3 \left(\frac{Q^2}{k} \right). \quad (31) \end{aligned}$$

The commonly accepted practice is to vary k in the interval $1/4 \leq k \leq 4$ (see, e. g., Ref. 69). We repeated our fits both without and with the IRR model of the twist-4 terms in the cases of $k = 1/4$ and $k = 4$. As in the fits described above, in order to achieve the minimum in χ^2 , we supplemented the interpolation procedure of the NNLO approximation for $\gamma_{F_3}^{(n)}(A_s)$ by fine-tuning of even terms $\gamma_{F_3}^{(2)}(6)$, $\gamma_{F_3}^{(2)}(8)$, and $\gamma_{F_3}^{(2)}(10)$ and got their values, comparable within small error-bars with the numbers given in Sec. 3. The same procedure was used in the process of the N³LO fits. In fact, they have more theoretical uncertainties than the NNLO ones. Indeed, in this case we applied the interpolation procedure to determine not only the NNLO coefficients of anomalous dimensions of even moments of x_{F_3} SF but the related N³LO terms of the coefficient functions as well (see Table 2). The N³LO corrections $r(n)$ to AD function in Eq. (30) were modelled using the [1/1] Padé approximant procedure. Note that, for even values of n , the numerical expressions for $q(n)$, which enter into the Padé approximants, are determined in part by the NNLO coefficients of anomalous dimensions of even moments of x_{F_3} . In the process of N³LO fits in the case of $k = 4$, the ambiguities of the applications of the [1/1] Padé approximation procedure reflect themselves in the necessity of supplementing the interpolation procedure by fine-tuning of the coefficient $\gamma_{F_3}^{(2)}(12)$ in addition to the $n = 6, 8, 10$ NNLO anomalous-dimension terms. Only after this additional step we were able to achieve a reasonable value of χ^2 in this case also.

The consequences of the study of factorization/renormalization scale dependence at the NLO, NNLO, and N³LO in the case of the initial scale $Q_0^2 = 20 \text{ GeV}^2$ are presented in Table 11.

It should be mentioned that despite the approximate nature of the Padé resummation procedure used for the estimation of the N³LO contribution $r(n)$ to the anomalous-dimension function AD , in the case of application of the fine-tuning procedure at $k = 1$ and $k = 1/4$, we get for $\gamma_{F_3}^{(2)}(n)$, with $n = 6, 8, 10, 12$, the numerical expressions which agree with the interpolated numbers of Table 1 in the 4th significant digit. For the fine-tuned fits with $k = 4$ and high-twist terms included, the price for small values of χ^2 is paid by more approximate determinations of $\gamma_{F_3}^{(2)}(10)$ and $\gamma_{F_3}^{(2)}(12)$, which differ from the ones presented in Sec. 3 in the 3rd significant digit. For example, for $n = 12$ the following number was obtained: $\gamma_{F_3}^{(2)}(12) \approx 1694.4907 \pm 3.1194$. It should be stressed, however, that this difference leads to negligibly small effects in the overall contributions to Padé estimated values of $r(n)$. Moreover, it is rather pleasant that the approximate character of the fixation of this part of the theoretical input of our new N³LO fits does not drastically spoil reasonable (from our point of view) estimates for $\gamma_{F_3}^{(2)}(n)$ at $n = 6, 8, 10, 12$.

We make now several conclusions which come from the results presented in Table 11.

Table 11. The outcomes of NLO, NNLO, and N³LO fits to CCFR'97 xF_3 data for $Q^2 \geq 5 \text{ GeV}^2$ with different values of factorization/renormalization scales. The difference in the values of $\Lambda_{\overline{MS}}^{(4)}$ is determined by $\Delta_k(\text{MeV}) = \Lambda_{\overline{MS}}^{(4)}(k) - \Lambda_{\overline{MS}}^{(4)}(k=1)$. The value of the IRR model coefficient is given in GeV^2 . The initial scale is fixed at $Q_0^2 = 20 \text{ GeV}^2$

Order	N_{\max}	k	$\Lambda_{\overline{MS}}^{(4)}$	Δ_k	A'_2 (HT)	χ^2/points
NLO	9	1	345 ± 38	—	—	85.1/86
	9	1	376 ± 39	—	-0.121 ± 0.052	79.5/86
	9	1/4	482 ± 57	137	—	90.0/86
	9	1/4	579 ± 62	203	-0.184 ± 0.054	78.8/86
	9	4	270 ± 25	-75	—	84.7/86
	9	4	271 ± 24	-105	-0.032 ± 0.051	84.4/86
NNLO	9	1	331 ± 37	—	—	75.8/86
	9	1	332 ± 36	—	-0.015 ± 0.051	75.7/86
	9	1/4	379 ± 45	47	—	78.7/86
	9	1/4	399 ± 46	66	-0.084 ± 0.052	76.1/86
	9	4	297 ± 27	-35	—	79.4/86
	9	4	318 ± 30	-15	$+0.117 \pm 0.052$	74.9/86
N ³ LO	9	1	327 ± 34	—	—	76.4/86
	9	1	329 ± 34	—	$+0.033 \pm 0.052$	76.0/86
	9	1/4	355 ± 39	28	—	75.9/86
	9	1/4	357 ± 39	28	-0.026 ± 0.051	75.9/86
	9	4	312 ± 24	-15	—	74.8/86
	9	4	318 ± 24	-11	$+0.058 \pm 0.052$	84.5/86

- At NLO, NNLO, and N³LO and $k = 1/4$ the values of $\Lambda_{\overline{MS}}^{(4)}$ and thus α_s are larger than in the case of $k = 1$, while for $k = 4$ smaller numbers are obtained.

- The NLO and NNLO results of Table 11 are in satisfactory agreement with the similar ones from Table 6 of Ref. 5, provided one takes into account the difference in the definitions of the parameter k (in [5] the case $k = 4$ ($k = 1/4$) corresponds to the choice $k = 1/4$ ($k = 4$) in Table 11).

- In our point of view, the results of the NNLO fits with $k = 1/4$ ($k = 4$) both without and with twist-4 terms simulate in part the results of the NLO (N³LO) fits with $k = 1$.

- The increase of order of perturbative-theory approximations leads to minimization of the scale-dependence uncertainty which manifests itself through the decrease of the values of Δ_k deviations.

- In the case of NLO fits with HT terms, the value of $|\Delta_k|$ is larger than in the case of switching of power-suppressed terms. However, this difference is

minimized at the NNLO and especially at the N³LO. We think that this property is reflecting the correlation with the effective minimization of the fitted value of the HT parameter A'_2 , which becomes comparable to zero in the NNLO and N³LO fits with $k = 1$.

- We checked that, for $k = 1$ and $k = 1/4$ the results are not sensitive to changes of the initial scale from $Q_0^2 = 20 \text{ GeV}^2$ to $Q_0^2 = 5 \text{ GeV}^2$.

- However, when $k = 4$, this pleasant feature is violated in the results of the NNLO and especially N³LO fits. Indeed, these fits are accompanied by the increase of χ^2 up to over the 100/86 level. This fact can be related to pushing the value of Q_0^2 out of the considered kinematical region $Q^2 \geq 5 \text{ GeV}^2$ (at $Q_0^2 = 5 \text{ GeV}^2$ and $k = 4$, the region of $1.25 \leq Q^2 \leq 5 \text{ GeV}^2$ should be also taken into account; however the NNLO and N³LO corrections to the coefficient functions are rather large in this region).

- It should be stressed that the NLO and NNLO results of Table 11 with $k = 4$ are closer to the ones obtained in the recent work of [37]. We will comment on the possible consequences of this observation in Sec. 5.2 below.

Let us now turn to determination of the values of $\alpha_s(M_Z)$ from the results of Table 11. We transform $\Lambda_{\overline{MS}}^{(4)}$ into $\Lambda_{\overline{MS}}^{(5)}$ using the NLO, NNLO, and N³LO variants of equation of Ref. 70:

$$\beta_0^{f+1} \ln \frac{\Lambda_{\overline{MS}}^{(f+1)2}}{\Lambda_{\overline{MS}}^{(f)2}} = (\beta_0^{f+1} - \beta_0^f) L_h + \delta_{\text{NLO}} + \delta_{\text{NNLO}} + \delta_{\text{N}^3\text{LO}}, \quad (32)$$

$$\delta_{\text{NLO}} = \left(\frac{\beta_1^{f+1}}{\beta_0^{f+1}} - \frac{\beta_1^f}{\beta_0^f} \right) \ln L_h - \frac{\beta_1^{f+1}}{\beta_0^{f+1}} \ln \frac{\beta_0^{f+1}}{\beta_0^f}, \quad (33)$$

$$\begin{aligned} \delta_{\text{NNLO}} = \frac{1}{\beta_0^f L_h} \left[\frac{\beta_1^f}{\beta_0^f} \left(\frac{\beta_1^{f+1}}{\beta_0^{f+1}} - \frac{\beta_1^f}{\beta_0^f} \right) \ln L_h + \right. \\ \left. + \left(\frac{\beta_1^{f+1}}{\beta_0^{f+1}} \right)^2 - \left(\frac{\beta_1^f}{\beta_0^f} \right)^2 - \frac{\beta_2^{f+1}}{\beta_0^{f+1}} + \frac{\beta_2^f}{\beta_0^f} - C_2 \right], \quad (34) \end{aligned}$$

$$\begin{aligned} \delta_{\text{N}^3\text{LO}} = \frac{1}{(\beta_0^f L_h)^2} \left[-\frac{1}{2} \left(\frac{\beta_1^f}{\beta_0^f} \right)^2 \left(\frac{\beta_1^{f+1}}{\beta_0^{f+1}} - \frac{\beta_1^f}{\beta_0^f} \right) \ln^2 L_h + \right. \\ \left. + \frac{\beta_1^f}{\beta_0^f} \left[-\frac{\beta_1^{f+1}}{\beta_0^{f+1}} \left(\frac{\beta_1^{f+1}}{\beta_0^{f+1}} - \frac{\beta_1^f}{\beta_0^f} \right) + \frac{\beta_2^{f+1}}{\beta_0^{f+1}} - \frac{\beta_2^f}{\beta_0^f} + C_2 \right] \ln L_h + \right. \end{aligned}$$

$$\begin{aligned}
& + \frac{1}{2} \left(- \left(\frac{\beta_1^{f+1}}{\beta_0^{f+1}} \right)^3 - \left(\frac{\beta_1^f}{\beta_0^f} \right)^3 - \frac{\beta_3^{f+1}}{\beta_0^{f+1}} + \frac{\beta_3^f}{\beta_0^f} \right) + \\
& \quad + \frac{\beta_1^{f+1}}{\beta_0^{f+1}} \left(\left(\frac{\beta_1^f}{\beta_0^f} \right)^2 + \frac{\beta_2^{f+1}}{\beta_0^{f+1}} - \frac{\beta_2^f}{\beta_0^f} + C_2 \right) - C_3 \Big], \quad (35)
\end{aligned}$$

where β_i^f (β_i^{f+1}) are the coefficients of the β function with f ($f+1$) numbers of active flavour; $L_h = \ln(M_{f+1}^2/\Lambda_{\overline{MS}}^{(f)2})$ and M_{f+1} is the threshold of the production of a quark of the $(f+1)$ flavour and $C_3 = -(80507/27648)\zeta(3) - (2/3)\zeta(2)((1/3)\ln 2 + 1) - 58933/124416 + (f/9)[\zeta(2) + 2479/3456]$. These formulae contain the NNLO correction to the matching condition with coefficient $C_2 = -7/24$, previously derived in Ref. 71 and correctly calculated in Ref. 72. In our massless analysis we will take $f = 4$ and $m_b \approx 4.8$ GeV and vary the threshold of the production of the fifth flavour from $M_5^2 \approx m_b^2$ to $M_5^2 \approx (6m_b)^2$ in accordance with the proposal of Ref. 73. The latter choice is based on the calculations of the LO and NLO massive corrections to the Gross–Llewellyn–Smith sum rule. The final values of $\alpha_s(M_Z)$ will be fixed at the middle of the interval, limited by the choices of threshold matching point at $M_5^2 \approx m_b^2$ and $M_5^2 \approx (6m_b)^2$. The appearing theoretical ambiguities reflect the uncertainties due to the manifestation of the massive-dependent contributions to the moments of xF_3 in the massless fits. Another procedure of fixing the massive-dependent ambiguities in $\alpha_s(M_Z)$, which result from the fits to xF_3 data, was proposed in Ref. 74. It is based on the application of the mass dependence of the LO contribution to β function in the MOM scheme, previously studied in the works of Refs. 75, 76. This procedure gives the estimates of the influence of mass dependence on the value of $\alpha_s(M_Z)$, extracted from CCFR'97 xF_3 data, which are comparable to ours. To be more complete at this point, we also mention several other works, which are dealing with different prescriptions for estimating threshold uncertainties (see Refs. 77, 78 and Ref. 79 especially, where mass dependence of the MOM-scheme coupling constant was evaluated at the 2-loop level). It was shown in Ref. 73 that the application of the \overline{MS} -scheme matching condition with the matching point $M_5^2 \approx (6m_b)^2$ does not contradict the application of the mass-dependent approach of Ref. 79. Therefore, we can conclude that our estimates of mass dependent uncertainties in $\alpha_s(M_Z)$ can be substantiated by this comparisons of the results of Refs. 73, 79.

Taking into account the numbers given in Table 11, which were obtained with the twist-4 contribution fixed using the IRR model of Ref. 29, and the theoretical expressions of Eqs. (14)–(16) and Eqs. (32)–(35), supplemented with the estimates of the uncertainties due to different possibilities of the choice of matching point and experimental systematic errors, which come from separate consideration of this type of experimental uncertainties of CCFR'97 data, we arrive at the following values of $\alpha_s(M_Z)$, extracted from the fits to CCFR'97

data for xF_3 performed in this work:

$$\begin{aligned} \text{NLO HT of Ref. 29 } \alpha_s(M_Z) &= 0.120 \pm 0.002(\text{stat.}) \pm 0.005(\text{syst.}) \pm \\ &\pm 0.002(\text{thresh.})_{-0.006}^{+0.010}(\text{scale}), \end{aligned} \quad (36)$$

$$\begin{aligned} \text{NNLO HT of Ref. 29 } \alpha_s(M_Z) &= 0.119 \pm 0.002(\text{stat.}) \pm 0.005(\text{syst.}) \pm \\ &\pm 0.002(\text{thresh.})_{-0.002}^{+0.004}(\text{scale}). \end{aligned} \quad (37)$$

Minor differences with the similar results of Ref. 5 are explained by the incorporation of more significant digits in the process of calculations and by more careful study of the scale-dependence uncertainties. These values presented in Eqs. (36), (37) should be compared with the one given by our new N³LO approximate fit:

$$\begin{aligned} \text{N}^3\text{LO HT of Ref. 29 } \alpha_s(M_Z) &= 0.119 \pm 0.002(\text{stat.}) \pm 0.005(\text{syst.}) \pm \\ &\pm 0.002(\text{thresh.})_{-0.001}^{+0.002}(\text{scale}). \end{aligned} \quad (38)$$

Note again, that the experimental systematic uncertainties are extracted from the CCFR'97 data and were not taken into account in the process of our concrete studies for the reasons discussed above. As to the theoretical uncertainties of the $\alpha_s(M_Z)$ value, the incorporation of the high-order corrections to the fits leaves threshold ambiguities at the same level, but decreases scale-dependence uncertainties drastically*.

To study the influence of the twist-4 contributions of Eq. (21) to the values of $\alpha_s(M_Z)$, we also extracted from Table 11 the corresponding results, obtained from the twist-4 independent fits to CCFR'97 data:

$$\begin{aligned} \text{NLO } \alpha_s(M_Z) &= 0.118 \pm 0.002(\text{stat.}) \pm 0.005(\text{syst.}) \pm \\ &\pm 0.002(\text{thresh.})_{-0.005}^{+0.007}(\text{scale}), \end{aligned} \quad (39)$$

$$\begin{aligned} \text{NNLO } \alpha_s(M_Z) &= 0.119 \pm 0.002(\text{stat.}) \pm 0.005(\text{syst.}) \pm \\ &\pm 0.002(\text{thresh.})_{-0.002}^{+0.003}(\text{scale}). \end{aligned} \quad (40)$$

*However, like in other studies of the CCFR'97 data of Refs. 3-5, 7, 37-39, 74, we are neglecting theoretical uncertainties, which arise from the separation from the CCFR'97 data heavy-nuclei corrections. Definite theoretical considerations of this problem [80,81] were incorporated in the fits in Ref. 82 and indicate the decrease of $\alpha_s(M_Z)$ at the NNLO level to the amount about $2 \cdot 10^{-3}$.

The approximate N³LO twist-independent fits give us the following numbers:

$$\begin{aligned} \text{N}^3\text{LO } \alpha_s(M_Z) = & 0.119 \pm 0.002(\text{stat.}) \pm 0.005(\text{syst.}) \pm \\ & \pm 0.002(\text{thresh.})_{-0.001}^{+0.002}(\text{scale}). \quad (41) \end{aligned}$$

Let us make several conclusions, which follow from the comparison of the results of Eqs. (36)–(40).

- In the case when HT corrections are included, the general tendency $(\alpha_s(M_Z))_{\text{NLO}} \geq (\alpha_s(M_Z))_{\text{NNLO}} \geq (\alpha_s(M_Z))_{\text{N}^3\text{LO}}$ for the central values of the outcomes of the fits takes place.

- The scale dependence of the NLO and NNLO results with HT corrections included are larger than in the case of $\alpha_s(M_Z)$ values, obtained without HT-terms.

- The scale dependence of the results of the approximate N³LO fits both without and with HT corrections is almost the same. This feature is related to effective minimization of the contributions of HT terms at the N³LO.

- Starting from the NNLO, the systematical experimental uncertainties dominate theoretical ambiguities as estimated by us.

- The uncertainties of the matching conditions dominate scale-dependence ambiguities at the N³LO only. This might mean that the approximation of massless quarks works reasonably well in the analysis of CCFR'97 xF_3 data up to NNLO.

It is worth making several comments on the comparison of our results for $\alpha_s(M_Z)$, extracted from the CCFR'97 xF_3 data, with those available in the literature. Within existing theoretical error bars, which reflect in part the special features of the procedures of taking into account threshold effects, our twist-independent NLO result is in agreement with the value $\alpha_s(M_Z)_{\text{NLO}} \approx 0.122 \pm 0.004$, given by the independent NLO fits to CCFR'97 xF_3 data using the Jacobi polynomial method [74]. It is also in agreement with the one presented by the CCFR collaboration, namely $\alpha_s(M_Z)_{\text{NLO}} = 0.119 \pm 0.002(\text{exp.}) \pm 0.004(\text{theor.})$ [7], which was obtained with the help of the DGLAP approach and reproduced in Ref. 38 without carefully treating theoretical uncertainties. Within experimental and theoretical error bars, our results also do not contradict the recent application of the Bernstein polynomial method [36] for the extraction of $\alpha_s(M_Z)$ from CCFR'97 xF_3 data at the NLO and NNLO [37]. Indeed, at the NLO it gives $\alpha_s(M_Z)_{\text{NLO}} = 0.116 \pm 0.004$, while at the NNLO they got $\alpha_s(M_Z) = 0.1153 \pm 0.0041(\text{exp.}) \pm 0.0061(\text{theor.})$ [37]. It is worth mentioning here that, despite the qualitative agreement with our results, the central values of $\alpha_s(M_Z)$ obtained in Ref. 37 are lower than the central values of all existing NLO and NNLO determinations of $\alpha_s(M_Z)$ from CCFR'97 xF_3 data. In Sec. 5 we will present a more detailed comparison of the results of Ref. 37 with the ones obtained in our work and will propose a possible explanation of the **origin** of these deviations.

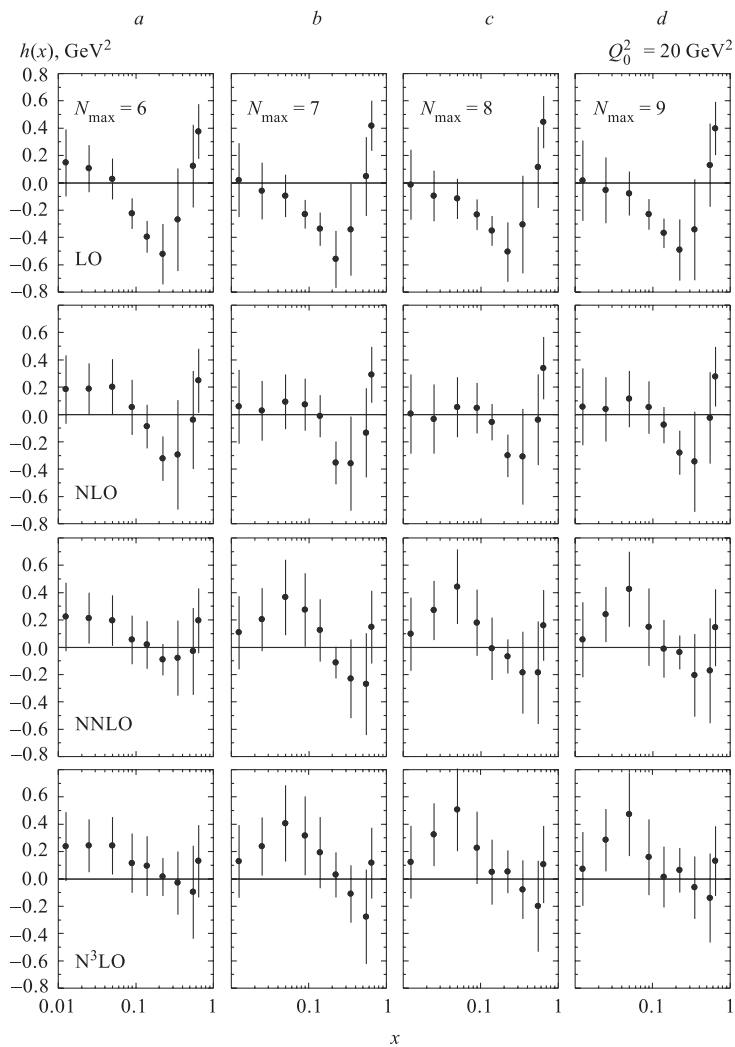
Although we do not include in our fits the simultaneous analysis of the statistical and systematic experimental uncertainties, we think that our analysis has some advantages over other fits to CCFR'97 xF_3 data. Indeed, the results of Refs. 74, 37 are free from considerations of the scale-dependence ambiguities studied in our work, while the DGLAP fits of the same data, performed in Refs. 7, 38, 39, do not take into consideration the contributions of the NNLO and N³LO perturbative QCD corrections, which we were able to treat in the way described above.

To our point of view, another advantage of our work is that using more **rigorous** information than previously (see Ref. 5) on the effects of the higher-order perturbative QCD contributions to the characteristics of xF_3 SF, we continued the studies of the influence of twist-4 corrections to the extraction of $\alpha_s(M_Z)$ from CCFR'97 xF_3 data. However, the IRR approach used by us is not the only way of modelling twist-4 effects. In the next Section, we are considering the case when the twist-4 contribution will be approximated in a less model-dependent way.

4.4. Determination of the x Shape of the Twist-4 Corrections. We now turn to a pure phenomenological extraction of the twist-4 contribution $h(x)$ to Eq. (18). In order to get its x dependence we will model $h(x)$ by free parameters $h_i = h(x_i)$, where x_i are the points in experimental data binning. The results are presented in Table 12.

The x shapes of $h(x)$, obtained at LO, NLO, NNLO and approximate N³LO, are depicted at the Figure, where we also illustrate the similar behaviour of $h(x)$, obtained in the cases of $N_{\max} = 6, 7, 8$, which correspond to smaller number of Mellin moments, used in the perturbative part of the Jacobi polynomial reconstruction formula of Eq. (18).

It should be noted that, to minimize correlations between the values of h_i , the parameters of the model for $xF_3(x, Q_0^2) = A(Q_0^2)x^{b(Q_0^2)}(1-x)^{c(Q_0^2)}(1+\gamma(Q_0^2)x)$ and the QCD scale $\Lambda_{\overline{MS}}^{(4)}$, we choose only 9 twist-4 parameters h_i , contrary to 16 ones considered in the process of our previous analysis of Refs. 3, 5. The results of the fits are presented in Table 12. The approximate N³LO fits are based on the application of available N³LO corrections to the coefficient functions of odd Mellin moments for xF_3 [23], supplemented with the smooth interpolation procedure (see Table 2) and using the [1/1] Padé model of the N³LO contributions $r(n)$ to the expanded anomalous-dimension term of Eq. (10) (see Table 3). In the process of NNLO and approximate N³LO fits we faced a problem identical to the one revealed while fitting xF_3 CCFR'97 data without twist-4 terms (see Sec. 3) and with twist-4 contributions, modelled by means of the IRR approach (see Eqs. (20), (21)). Indeed, to get the stable value of χ^2 at $N_{\max} = 9$ it was necessary to apply the fine-tuning procedure for the NNLO corrections to $\gamma_{F_3}^{(n)}$ at $n = 6, 8, 10, 12$. The obtained values of these parameters are presented in Table 12 also. Within error bars, they are in agreement with the numbers fixed by the smooth interpolation procedure (see Table 1).



The x shapes of $h(x)$ extracted from the fits to xF_3 CCFR'97 data in different orders of perturbative theory. The initial scale is chosen at $Q_0^2 = 20 \text{ GeV}^2$. The cases of different N_{max} are considered: a) $N_{\text{max}} = 6$; b) $N_{\text{max}} = 7$; c) $N_{\text{max}} = 8$; d) $N_{\text{max}} = 9$

Several comments are now in order.

1. The obtained values of χ^2 , given in Table 12, are considerably smaller than the ones obtained in the process of the fits without twist-4 contributions (see Table 4) and with $1/Q^2$ terms modelled through the IRR approach

Table 12. The values of the parameters $h(x_i)$, A , b , c , γ and $\Lambda_{\overline{MS}}^{(4)}$ with corresponding statistical errors. They are obtained from the fits with $N_{\max} = 9$ and $Q_0^2 = 20 \text{ GeV}^2$

	LO	NLO	NNLO	N ³ LO
χ^2/nep	69.1/86	68.5/86	65.6/86	66.1/86
A	4.32 ± 1.34	4.08 ± 1.13	5.06 ± 0.46	5.55 ± 1.27
b	0.629 ± 0.096	0.616 ± 0.084	0.682 ± 0.030	0.711 ± 0.079
c	4.28 ± 0.14	4.16 ± 0.15	3.88 ± 0.20	3.73 ± 0.34
γ	1.91 ± 1.20	1.87 ± 1.09	0.73 ± 0.30	0.25 ± 0.81
$\Lambda_{\overline{MS}}^{(4)}$, MeV	327 ± 149	395 ± 151	391 ± 159	370 ± 131
$\alpha_s(M_Z)$	$0.140^{+0.010}_{-0.010}$	$0.123^{+0.007}_{-0.007}$	$0.124^{+0.008}_{-0.010}$	$0.123^{+0.007}_{-0.008}$
x_i	$h(x_i)$, GeV ²			
0.0125	0.016 ± 0.295	0.056 ± 0.281	0.054 ± 0.274	0.072 ± 0.271
0.025	-0.055 ± 0.241	0.038 ± 0.235	0.239 ± 0.203	0.284 ± 0.228
0.050	-0.079 ± 0.161	0.113 ± 0.206	0.425 ± 0.275	0.472 ± 0.306
0.090	-0.231 ± 0.112	0.050 ± 0.193	0.146 ± 0.283	0.158 ± 0.277
0.140	-0.369 ± 0.108	-0.078 ± 0.132	-0.012 ± 0.211	0.013 ± 0.223
0.225	-0.492 ± 0.223	-0.281 ± 0.160	-0.038 ± 0.123	0.062 ± 0.163
0.350	-0.344 ± 0.371	-0.347 ± 0.367	-0.207 ± 0.303	-0.064 ± 0.227
0.550	0.129 ± 0.304	-0.026 ± 0.335	-0.172 ± 0.385	-0.140 ± 0.325
0.650	0.398 ± 0.195	0.275 ± 0.219	0.144 ± 0.282	0.131 ± 0.255
n			$\gamma_{F_3}^{(2)}(n)$	$\gamma_{F_3}^{(2)}(n)$
6			1247.9 ± 0.7	1247.7 ± 0.6
8			1419.9 ± 0.8	1419.9 ± 0.8
10			1561.9 ± 2.2	1561.6 ± 2.2
12			1676.7 ± 5.3	1676.8 ± 4.9

(see Table 6). This is the welcome feature of the analysis of DIS data, which is based on the model-independent parameterization of the twist-4 terms.

- The parameters A , b , c , γ and $\Lambda_{\overline{MS}}^{(4)}$ given in Table 12 are in agreement with their values, obtained in Ref. 5 with the help of the fits, which were made in the case of $N_{\max} = 6$ and 16 HT parameters h_i .
- Due to the effect of correlations of h_i and $\Lambda_{\overline{MS}}^{(4)}$ the values of the QCD scale parameter have rather large statistical error bars.
- At the LO and NLO the x shape for $h(x)$ is rather stable to the increase of N_{\max} from $N_{\max} = 6$ to $N_{\max} = 9$ and, therefore, to the incorporation of the additional Mellin moments in the procedure of reconstruction of xF_3 via the Jacobi polynomial technique.
- The x shape of $h(x)$, obtained at the LO and NLO, is in agreement with the prediction of the IRR model of Ref. 29.

6. At the NNLO, we observe the sinusoidal-type oscillations of $h(x)$, which are becoming more vivid in the cases of $N_{\max} = 8$ and $N_{\max} = 9$.
7. This feature seems to be in agreement with the qualitative expectations which result from an educated guess about the possible modifications of the prediction of the IRR model at the NNLO [83].
8. At the N³LO, for all considered N_{\max} , the shapes of $h(x)$ are similar to the ones obtained in the process of new NNLO fits.
9. It is worth mentioning that the positive bumps in the $x < 0.1$ region of the NNLO plots of the Figure appear after applying the fine-tuning procedure to NNLO coefficients of $\gamma_{F_3}^{(n)}$ for $n = 6, 8, 10, 12$, which gives us the possibility of getting reasonable values for both χ^2 and $\Lambda_{\overline{MS}}^{(4)}$ at NNLO and beyond. In other words, the x profile of the twist-4 contribution is related to the values of the NNLO corrections to $\gamma_{F_3}^{(n)}$ for even n . We consider this observation as an additional argument in favour of getting explicit results for these terms.
10. In general, taking into account systematic experimental uncertainties of the CCFR'97 data for xF_3 might make the sinusoidal-type oscillations of $h(x)$, which demonstrate themselves in the NNLO and approximate N³LO fits with smaller number of free parameters h_i , less vivid and more comparable with zero. Indeed, the effective minimization observed previously in Refs. 3, 5 of the contribution of twist-4 terms during less definite than the present NNLO fits to xF_3 CCFR'97 data were confirmed in the process of the NNLO DGLAP fits to F_2 data for charged leptons DIS [84, 85], which were based on the application of the approximate NNLO model for the DGLAP kernel from Ref. 69. The observed changes in the x shape of twist-4 contributions $h(x)$ to xF_3 and F_2 SFs serve as additional arguments in favour of high-twist duality, which demonstrates itself through the interplay between NNLO perturbative QCD corrections and $1/Q^2$ terms.
11. It is interesting to note, that large α_s associated with considerable twist-4 contributions was revealed some time ago in the process of NLO DGLAP fits of other νN DIS data [86]. Note, however, that in this work twist-4 contributions were not free, as in our analysis, but were simulated using special model.

5. COMPARISON WITH THE RESULTS OF OTHER NNLO ANALYSES

In this Section, we compare the results of our studies with the outcomes of other analyses of xF_3 at the NLO and beyond, performed independently in Refs. 35 and 37.

In Ref. 35, to study the evolution of the NS contributions to F_2 and xF_3 up to the approximate N³LO level of massless QCD, the NNLO corrections to the DGLAP equation coefficient functions for xF_3 [13] and the N³LO corrections to definite Mellin moments of NS SFs, obtained in Refs. 20, 23, were combined with the NNLO model for the NS kernel, previously obtained in Ref. 69.

5.1. Comments on Estimates of Scale-Scheme Dependence Uncertainties.

Using the input

$$F_{2,\text{NS}}(x, Q_0^2) = xF_3(x, Q_0^2) = x^{0.5}(1-x)^3 \quad (42)$$

specifying the reference scale Q_0^2 through the normalization condition $\alpha_s(\mu_R^2 = Q_0^2 = 30 \text{ GeV}^2) = 0.2$, irrespective of the order of the expansion and varying the renormalization scale in the conventional interval $\frac{1}{4}Q^2 \leq \mu_R^2 \leq 4Q^2$, the authors of Ref. 35 studied the effects of the scaling violation using a definite model for the xF_3 data. The values of $\alpha_s(30 \text{ GeV}^2)$ for $f = 4$ are given in the second column of Table 13. However, while analyzing real CCFR'97 xF_3 data, we found that scale-dependent uncertainties can be larger. Indeed, using those numbers from Table 11, which are related to twist-independent fits to the CCFR'97 data, we obtain the inputs in the third column of Table 13.

Table 13. The comparison of the scale uncertainties of $\alpha_s(30 \text{ GeV}^2)$, obtained in Ref. 35 and in the process of our studies

Order	Values from Ref. 35	Our values
NLO	$0.2035^{+0.019}_{-0.011}$	$0.2104^{+0.0252}_{-0.0151}$
NNLO	$0.1995^{+0.0065}_{-0.0015}$	$0.2148^{+0.0097}_{-0.0072}$
N ³ LO	$0.2000^{+0.0025}_{-0.0005}$	$0.2144^{+0.0058}_{-0.0032}$

At the qualitative level, both sets of numbers are in agreement with each other. Moreover, the scale-dependence of both sets of numbers has the tendency to decrease from NLO up to N³LO. Definite differences between the central values of α_s may be traced to the fact that our results for $\alpha_s(30 \text{ GeV}^2)$ correspond to $\alpha_s(M_Z) \approx 0.118$ irrespective of the order of the expansion (see Eqs. (39)–(41)), while the choice $\alpha_s(30 \text{ GeV}^2) = 0.2$ in Ref. 35 corresponds to a lower value $\alpha_s(M_Z) \approx 0.116$.

On the other hand, the scale dependence of our twist-independent NLO and NNLO results for $\alpha_s(M_Z)$ (see Eqs. (39), (40)) is in agreement with the previous estimates of this kind of theoretical uncertainties, namely

$$\Delta\alpha_s(M_Z)_{\text{NLO}} = {}^{+0.006}_{-0.004}, \quad \Delta\alpha_s(M_Z)_{\text{NNLO}} = {}^{+0.0025}_{-0.0015}, \quad (43)$$

obtained in Ref. 69 using the model constructed in this work for the NNLO NS DGLAP kernel.

As to the application in Ref. 69 of the renormalization-scheme optimization methods of Refs. 48, 87 for estimating higher-order corrections (up to N⁴LO) to the factorization-scheme-independent quantity, defined as

$$K_n(Q^2) = -2 \frac{d \ln M_n^{F_3}}{d \ln Q^2} = \gamma_{F_3}^{(n)}(A_s) - \beta(A_s) \frac{\partial C_{F_3}^{(n)}(A_s)/\partial A_s}{C_{F_3}(A_s)}, \quad (44)$$

we think that it might give larger theoretical uncertainties than those presented in Ref. 69. Indeed, we previously used this ratio in Ref. 5 in the process of attempting to perform the massless NNLO fits to CCFR'97 xF_3 data using the effective-charges (ECH) approach of Ref. 88 (for the related methods see Refs. 89–92 and the independent unpublished proposal of Ref. 93; for the related phenomenological applications in the NLO fits to the charged leptons DIS SFs data, see Ref. 94). As was found in Ref. 5, the NNLO ECH fits to CCFR'97 xF_3 data face the problem of the *drastical increase* of χ^2 up to the level of $\chi^2 \sim 111/86$. This effect was explained by the appearance of *large* and *negative* values of the NNLO coefficients $\tilde{\beta}_2^{(n)}$ of the ECH β functions, related to the scheme-invariant quantities introduced within the context of the principle of minimal sensitivity (PMS) [95]. Here we are going to demonstrate explicitly how this effect appears, using the results presented in Sec. 2.

In the case of $n \geq 2$, the NNLO approximation of the factorization-scheme independent kernel K_n can be rewritten in the following form:

$$R_n = \frac{K_n}{\gamma_{F_3}^{(0)}(n)} = A_s + d_1(n)A_s^2 + d_2(n)A_s^3. \quad (45)$$

Putting $d_1(n) = d_2(n) = 0$ we arrive at the following renormalization-group equation:

$$\left(\mu \frac{\partial}{\partial \mu} + \beta_{\text{eff}}^{(n)}(R_n) \frac{\partial}{\partial R_n} \right) R_n = 0, \quad (46)$$

with the effective β -function defined as

$$\mu \frac{\partial R_n}{\partial \mu} = \beta_{\text{eff}}^{(n)}(R_n) = -2 \left(\beta_0 R_n^2 + \beta_1 R_n^3 + \tilde{\beta}_2^{(n)} R_n^4 \right), \quad (47)$$

where the NNLO coefficient of Eq. (47) is related to the NNLO coefficients β_2 of the \overline{MS} -scheme β -function as

$$\tilde{\beta}_2^{(n)} = \beta_2 + \Delta(n) \quad (48)$$

with

$$\Delta(n) = \beta_0 \left(d_2(n) - \Omega_2(n) \right) \quad (49)$$

and

$$\Omega_2(n) = d_1(n) \left(\frac{\beta_1}{\beta_0} + d_1(n) \right). \quad (50)$$

The similar equations can be derived at the N³LO and beyond (see Refs. 48, 87).

The ECH-inspired estimates proposed in Refs. 48, 87 work only in the case when the differences $\tilde{\beta}_k^{(n)} - \beta_k$ with $k \geq 2$ are small. These conditions turned out to be valid for the e^+e^- -annihilation Adler D -function, DIS sum rules in QCD [48] and also $(g-2)_\mu$ in QED [87]. But, unfortunately, they are not working in the case of the quantity defined by Eq. (45). Indeed, using the results from Tables 1, 2 we obtain the numerical expressions for $\Delta(n)$, which are presented in Table 14.

Table 14. The n dependence of $\Delta(n) = \tilde{\beta}_2^{(n)} - \beta_2$ for $f = 4$

n	2	3	4	5	6	7	8	9	10	11	12	13
$\Delta(n)$	-1976	-1288	-1066	-937	-851	-783	-730	-684	-644	-606	-576	-547

Comparing now these numbers with the numerical value for β_2 for $f = 4$, ($\beta_2 = 406.35$), we arrive at the conclusion that the basic assumption of the ECH-inspired estimates of Refs. 48, 87, namely $\tilde{\beta}_2^{(n)} \approx \beta_2$, does not work at NNLO, not only in the previously considered case of the correlator of scalar quark currents [54], but for the factorization-scheme-independent quantity of Eq. (46) as well.

Despite the fact that we did not consider the case of $F_{2,\text{NS}}$ SF in detail, we think that the estimates (presented in Ref. 35) of perturbative theoretical uncertainties for the factorization-scheme independent kernel K_n for $F_{2,\text{NS}}$ made with the help of the ECH and PMS approaches at the NNLO and beyond, might be underestimated (at least in the case of $n \leq 13$). However, the general tendency of the absolute value of $\Delta(n)$ to decrease with increasing n might lead to the improvement of the situation for a larger number of moments, which are limited in Ref. 35 by $n = 30$. This guess can be substantiated only after completing the **explicit** analytical calculations of NNLO corrections to DGLAP kernels.

Another interesting subject, related to *negative* values of $\tilde{\beta}_2^{(n)}$, corresponds to the appearance of perturbative IRR zeros of the ECH β function at the NNLO, considered previously as spurious ones in a number of works (see Refs. 54, 96–99). It should be stressed, that, for the quantity K_n , these perturbative IRR zeros

are manifesting themselves obviously in the case of $n = 2$ and less obviously for $n = 3$. In the first case, the critical value of the corresponding effective charge $(\alpha_s)_{\text{eff}}$ is small, namely 0.4, while for $n = 3$ it is over 0.7, which is rather close to the nonperturbative region. For $n \geq 4$, these zeros lie in the typical nonperturbative sector, where $(\alpha_s)_{\text{eff}} \geq 1$. In view of this, it might still be possible to apply the ECH or PMS approaches for the analysis of the scheme-dependence of the NNLO perturbative QCD predictions for xF_3 moments with $n \geq 3$. It could be of interest to study this problem in the future.

5.2. Comments on Outputs of the NNLO Bernstein Polynomial Analyses.

Let us now comment on the comparison of our NLO and NNLO results for $\Lambda_{\overline{MS}}^{(4)}$ and $\alpha_s(M_Z)$ with the ones obtained in another interesting work [37]. The authors of this work used the theoretical input identical to ours, namely — the results of the NNLO perturbative QCD calculations for the anomalous dimensions and coefficient functions of odd Mellin moments of xF_3 , and performed the NLO and NNLO fits to CCFR'97 data for xF_3 with the help of the Bernstein polynomial technique, proposed in Ref. 36. In the process of these fits, the initial parameterization $xF_3(Q_0^2) = Ax^b(1-x)^c$, which is similar to Eq. (6), was considered. The initial scales $Q_0^2 = 8.75$ and 12 GeV^2 were chosen inside the kinematical region of CCFR'97 data $7.9 \leq Q^2 \leq 125.9 \text{ GeV}^2$, which is only part of the region used in our work.

The results of twist-independent fits at the scale $Q_0^2 = 8.75 \text{ GeV}^2$ obtained in Ref. 37 are summarized in the last two columns of Table 15, where the error bars include statistical and systematic experimental uncertainties.

These results can be compared with our outputs in Table 4, which result from our Jacobi polynomial twist-4 independent fits of the CCFR'97 data for xF_3 in the kinematical region $Q^2 \geq 5 \text{ GeV}^2$ with the cuts $W > 10 \text{ GeV}^2$, $x < 0.7$. It should be stressed that this region is identical to the one studied in the original work of the CCFR collaboration [7]. In particular, we are interested in the following values of $\Lambda_{\overline{MS}}^{(4)}$:

$$\begin{aligned}
 \text{LO} \quad \Lambda_{\overline{MS}}^{(4)} &= 265 \pm 36 \text{ MeV}, \\
 \text{NLO} \quad \Lambda_{\overline{MS}}^{(4)} &= 347 \pm 37 \text{ MeV}, \\
 \text{NNLO} \quad \Lambda_{\overline{MS}}^{(4)} &= 332 \pm 35 \text{ MeV},
 \end{aligned}
 \tag{51}$$

which correspond to the choice of the initial scale $Q_0^2 = 8 \text{ GeV}^2$ (note that the results of Table 4 demonstrate that these values are almost independent of the choice of Q_0^2).

It is quite understandable why our results have smaller error-bars: contrary to the results of Ref. 37, they are defined by the statistical experimental errors of

CCFR'97 data alone. However, the explanation of the discrepancies in the central values of $\Lambda_{\overline{MS}}^{(4)}$ is not so obvious.

In order to clarify the situation, we performed the Jacobi polynomial fits for two sets of experimental data from the CCFR'97 collaboration, choosing the same initial scale $Q_0^2 = 8.75 \text{ GeV}^2$ as in Ref. 37.

1. First, we considered the same data set as in Ref. 37, i. e., the kinematical region $7.9 \leq Q^2 \leq 125.9 \text{ GeV}^2$.

- The comparison of the results of our twist-4 independent fits with the ones given in Table 3 of Ref. 37 is presented in Table 15 below.

Table 15. The values of $\Lambda_{\overline{MS}}^{(4)}$ and $\alpha_s(M_Z)$, obtained with the help of Jacobi and Bernstein polynomial techniques $Q_0^2 = 8.75 \text{ GeV}^2$

Order	$\Lambda_{\overline{MS}}^{(4)}$	$\alpha_s(M_Z)$	χ^2/nep	$\Lambda_{\overline{MS}}^{(4)}$ [37]	$\alpha_s(M_Z)$ [37]
LO	227 ± 37	0.1309 ± 0.0037	92/74	217 ± 78	0.130 ± 0.006
NLO	298 ± 38	0.1169 ± 0.0025	76/74	281 ± 57	0.116 ± 0.004
NNLO	303 ± 38	0.1187 ± 0.0026	65/74	255 ± 55	0.1153 ± 0.0041

Notice that the difference between the values of $\Lambda_{\overline{MS}}^{(4)}$ obtained by the Jacobi and Bernstein polynomial techniques are minimized in this case. The LO and NLO results for $\alpha_s(M_Z)$, as obtained by us, almost coincide with those taken from Ref. 37. However, at the NNLO, our value of $\alpha_s(M_Z)$, which is in agreement with the result of Eq. (40), is comparable with the similar one given in Ref. 37 only within the presented experimental error bars, which in the latter case also include systematical experimental uncertainties.

- To perform a more detailed comparison we also estimated the uncertainties in the extraction of $\Lambda_{\overline{MS}}^{(4)}$ at the NNLO, as those considered in Table 4 of Ref. 37. The results are given in Table 16.

In this Table we mark by the symbol NNLO* the uncertainties of $\Lambda_{\overline{MS}}^{(4)}$, obtained from the NNLO fits with α_s defined through its N³LO expression (see Eqs. (14)–(16)). One can see that we obtained twice as small uncertainties while neglecting TMC and five times smaller effects while introducing the N³LO expression for α_s in the NNLO fits. It should be stressed that the similar small difference between the values of $\Lambda_{\overline{MS}}^{(4)}$ of the NNLO and NNLO* fits to the CCFR'97 xF_3 data was already observed in Ref. 5 for a larger kinematical region and for different values of Q_0^2 .

- At present we are unable to explain the most significant differences with the NNLO results of Ref. 37. We think that more detailed comparison of the Jacobi and Bernstein polynomial approaches at the NNLO is really on the agenda.

Table 16. Theoretical uncertainties of $\Lambda_{\overline{MS}}^{(4)}$, obtained with the help of Jacobi and Bernstein polynomial techniques $Q_0^2 = 8.75 \text{ GeV}^2$

Source of errors	$\Lambda_{\overline{MS}}^{(4)}$	$\Delta\Lambda_{\overline{MS}}^{(4)}$	$\Lambda_{\overline{MS}}^{(4)}$ [37]	$\Delta\Lambda_{\overline{MS}}^{(4)}$ [37]
No TMC	326	23	298	43
HT	316	13	270	15
Q_0^2 to 12 GeV^2	298	-5	263	-8
NNLO*	294	-9	209	-46

Table 17. The results of the fits to the CCFR'97 data within the kinematical conditions, used in our work. $Q_0^2 = 8.75 \text{ GeV}^2$

Order	$\Lambda_{\overline{MS}}^{(4)}$	$\alpha_s(M_Z)$	χ^2/nep
LO	265 ± 36	$0.1345^{+0.0031}_{-0.0033}$	113/86
NLO	340 ± 37	$0.1193^{+0.0021}_{-0.0023}$	87/86
NNLO	333 ± 36	$0.1206^{+0.008}_{-0.0020}$	74/86
NNLO no TMC	360 ± 32	$0.1123^{+0.0018}_{-0.0020}$	77/86
NNLO*	322 ± 35	$0.1199^{+0.0021}_{-0.0022}$	74/86

2. If, following the CCFR collaboration, we exclude one data point with $W^2 < 10 \text{ GeV}^2$ (namely, the point with $x = 0.65$ and $Q^2 = 12.6 \text{ GeV}^2$), which has a large systematical error, and if we take into account the complete data set with $Q^2 \geq 5 \text{ GeV}^2$ and the cut $W^2 > 10 \text{ GeV}^2$, we reproduce the results of Eq. (51) with rather small theoretical uncertainties.

It is worth noting that theoretical uncertainties due to the omission of TMC and due to the consideration of the N³LO expression for α_s , Eqs. (14)–(16), in the NNLO fits remain the same as in the case of Table 16.

Several additional comments are now in order.

- In Table 15 and Table 17 the values of $\alpha_s(M_Z)$ were obtained from Eqs. (32)–(34) using the matching point $M_5 = m_b \approx 4.8 \text{ GeV}$. Thus we neglected the uncertainties due to fixation of b -quark threshold ambiguities, described in Sec. 4.3.

- Note, however, that our estimate $(\Delta\alpha_s(M_Z))_{\text{thresh}} \approx \pm 0.0017$ is only slightly larger than the estimate $(\Delta\alpha_s(M_Z))_{\text{thresh}} \approx 0.0010$, given in Ref. 37 after application of a different method for estimating b -quark threshold uncertainties.

- It should be noted that, contrary to the analysis in Ref. 37, we were able to study the scale-dependence uncertainties of our results in the case when the renormalization scale was taken equal to the factorization scale. The results of our studies, presented in Sec. 4.3 and Table 11, demonstrate the following interesting feature: in the case of $k = 4$ and HT neglected, both NLO and NNLO results

for $\Lambda_{\overline{MS}}^{(4)}$ are **almost identical** to the ones obtained in Ref.37 in a narrower kinematical region of CCFR'97 xF_3 data. Therefore, a possible explanation of the deviations of our results from the ones in Ref.37 might be related to the fact that scale-dependence ambiguities of the latter were not studied and might increase the theoretical uncertainty for $\alpha_s(M_Z)$.

5.3. The Model Independence of High-Twist Duality Effect. Despite the fact that in Ref.37 the subject related to the inclusion of twist-4 terms was briefly considered at the NNLO only, it is rather instructive to perform a similar analysis at the LO, NLO and repeat the NNLO studies using the Jacobi polynomial approach. It should be mentioned that in Ref.37 the more simple than IRR-model form of the twist-4 corrections was used, namely

$$M_{n,xF_3}^{\text{HT}}(Q^2) = n \frac{B'_2}{Q^2} M_n^{F_3}(Q^2), \quad \text{with } B'_2 = a(\Lambda_{\overline{MS}}^{(4)})^2. \quad (52)$$

Its coefficient function differs from $\tilde{C}(n)$ of Ref.29 (see Eq. (21)), which, for the moments under consideration, has the following numerical values: $\tilde{C}(2) = 1.6667$, $\tilde{C}(3) = 1.6333$, $\tilde{C}(4) = 1.4$, $\tilde{C}(5) = 1.0381$, $\tilde{C}(6) = 0.5857$, $\tilde{C}(7) = 0.0659$, $\tilde{C}(8) = -0.5063$, $\tilde{C}(9) = -1.1205$, $\tilde{C}(10) = -1.7689$ and $\tilde{C}(11) = -2.4461$, etc. Notice that, starting from $n=8$, $\tilde{C}(n)$ changes the sign and in the asymptotic regime tends to $-n$. Therefore, it is of interest to investigate the model-dependence of the effect observed in Sec.4.1 of high-twist duality using the HT model of Eq. (53), which is different from the IRR model of Ref.29.

This question was studied by us using the set of CCFR'97 xF_3 data considered in item (1) of Sec.5.2. The results, obtained with the help of Jacobi polynomial fits, are presented in Table 16, where b -quark threshold uncertainties were not taken into account. Note that, in our fits, we considered B'_2 as the free parameter and then determined the value of the parameter a , considered to be free in the fits of Ref.37.

Table 18. The results of the fits to the subset of CCFR'97 data with HT contribution, considered in Ref.37. The initial scale is chosen as $Q_0^2 = 8.75 \text{ GeV}^2$

Order	$\Lambda_{\overline{MS}}^{(4)}$	χ^2/nep	B'_2	a	$\alpha_s(M_Z)$
LO	433 ± 89	88/74	-0.330 ± 0.126	-1.76 ± 0.37	$0.1471^{+0.0056}_{-0.0063}$
NLO	371 ± 72	75/74	-0.135 ± 0.113	-0.98 ± 0.57	$0.1213^{+0.0039}_{-0.0044}$
NNLO	316 ± 51	64/74	-0.031 ± 0.088	-0.31 ± 0.80	$0.1195^{+0.0039}_{-0.0044}$

Comparing now Table 18 with Table 6 of Sec.3 we arrive at the following observations:

- In both cases the values of $\Lambda_{\overline{MS}}^{(4)}$ are almost the same and thus do not depend on the typical structure of the twist-4 model.

- At LO and NLO the value of the parameter B'_2 is in agreement with the value of the parameter A'_2 of the IRR model and decreases after NLO effects are taken into account.
- At NNLO the value of the parameter B'_2 is a bit larger than the similar value of A'_2 , but within error bars both are compatible with zero.
- At NNLO the central value for the parameter a is a bit larger than its value obtained in Ref. 37, but within existing uncertainties they are compatible.
- The effect observed in Sec. 4.1 of interplay between perturbative QCD and twist-4 corrections also remains valid in the case of the choice of twist-4 model given by Eq. (52).

CONCLUSIONS

In this work, we used the new perturbative QCD input in the form of NNLO corrections to the anomalous dimensions and N³LO corrections to the coefficient functions for odd xF_3 moments [23] to improve previous fits to xF_3 CCFR'97 data, performed in Refs. 3, 5. We demonstrated that the application of the smooth interpolation procedure, supplemented with the fine-tuning of NNLO corrections to $\gamma_{F_3}^{(n)}$ for several even n , gives us the chance to include in the NNLO and approximate N³LO fits a greater number of Mellin moments up to $n \leq 13$. The basic feature which we revealed in the process of our fits is the drastical reduction of the scale-dependence uncertainties for $\alpha_s(M_Z)$ at the NNLO and beyond. The obtained values of $\alpha_s(M_Z)$ turned out to be in agreement with the world average value of this parameter, namely $\alpha_s(M_Z) \approx 0.118$ [100, 101]. The previously discovered property of interplay between NNLO perturbative QCD corrections and twist-4 terms is confirmed using different models for the $1/Q^2$ corrections.

As to the effective decrease of the twist-4 contributions at the NNLO and beyond, we are unable to disfavour the possibility that it occurs because of the use of the CCFR'97 data for xF_3 , which are still not precise enough. Possible future more detailed DIS νN data, which are expected to be obtained at the Neutrino factory [102], might be useful for clarification of whether it is reliable to detect more clear signals from twist-4 contributions at the NNLO level.

On the other hand, our NNLO Jacobi polynomial fits revealed the necessity of getting more precise (namely exact) values for the NNLO corrections to the anomalous dimensions $\gamma_{F_3}^{(n)}$ for even n , which are related to still explicitly uncalculable NNLO corrections to the kernel of the DGLAP equation for xF_3 . Having this information at hand, one might be able to perform NNLO Jacobi polynomial fits avoiding interpolation and fine-tuning procedures, which were used by us to fix NNLO corrections to $\gamma_{F_3}^{(n)}$ for even n , and fix still remaining theoretical uncertainties in the x shape of HT contribution to xF_3 , extracted at the NNLO. More

detailed understanding of other physical effects when using explicit NNLO corrections to the kernels of the DGLAP equations might be revealed in the process of more detailed comparisons between different methods, which implement the classical DGLAP solution of differential equations in the x space and the Jacobi and Bernstein polynomial techniques.

Acknowledgements. It is a pleasure to thank S. I. Alekhin, G. Altarelli, S. Catani, J. Ellis, S. A. Larin, R. Lednicky, A. Petermann, A. A. Pivovarov, G. Salam, J. Santiago, D. V. Shirkov, W. van Neerven, A. Vogt and F. J. Yndurain for their interest in our work and constructive questions and comments.

We are grateful to B. I. Ermolaev, S. Forte, M. Greco and A. V. Kotikov for discussions of different subjects related to the behaviour of the NS SFs at small x .

The essential part of this work was done when one of us (A. K.) was visiting the Theory Division of CERN. The work of one of us (G. P.) was supported by Xunta de Galicia (PGIDT00PX20615PR) and CICYT (AEN99-0589-C02-02). From the Russian side, the work was supported by RFBR (Grants No. 02-01-00601, 00-02-17432). The work of A. V. S. was also supported by INTAS call 2000 (project No. 587). While in Russia the work of A. L. K. was done within the framework of State Support of Leading Scientific Schools (RFBR Grant No. 00-15-96626).

REFERENCES

1. Kataev A. L. *et al.* // Phys. Lett. B. 1996. V. 388. P. 179.
2. Sidorov A. V. // Phys. Lett. B. 1996. V. 389. P. 379.
3. Kataev A. L. *et al.* // Phys. Lett. B. 1998. V. 417. P. 374.
4. Kataev A. L., Parente G., Sidorov A. V. // Nucl. Phys. A. 2000. V. 666–667. P. 184.
5. Kataev A. L., Parente G., Sidorov A. V. // Nucl. Phys. B. 2000. V. 573. P. 405.
6. Kataev A. L., Parente G., Sidorov A. V. // Proc. of Intern. Bogoliubov Conf. on Problems of Theoretical and Mathematical Physics, Sept. 27–Oct. 6, 1999. FECA Y. 2000. V. 31, No. 7. P. 29; hep-ph/0001096.
7. Seligman W. G. *et al.* (CCFR-NuTeV Collaboration) // Phys. Rev. Lett. 1997. V. 79. P. 1213.
8. Parisi G., Sourlas N. // Nucl. Phys. B. 1979. V. 151. P. 421.
9. Barker I. S., Langensiepen C. B., Shaw G. // Nucl. Phys. B. 1981. V. 186. P. 61.
10. Chýla J., Ramez J. // Z. Phys. C. 1986. V. 31. P. 151.
11. Krivokhizhin V. G. *et al.* // Z. Phys. C. 1987. V. 36. P. 51.
12. Krivokhizhin V. G. *et al.* // Z. Phys. C. 1990. V. 48. P. 347.
13. Zijlstra E. B., van Neerven W. L. // Phys. Lett. B. 1992. V. 297. P. 377.
14. Moch S., Vermaseren J. A. M. // Nucl. Phys. B. 2000. V. 573. P. 853; hep-ph/9912355.
15. Gribov V. N., Lipatov L. N. // Sov. J. Nucl. Phys. 1972. V. 15. P. 438.
16. Lipatov L. N. // Sov. J. Nucl. Phys. 1975. V. 20. P. 94.

17. Altarelli G., Parisi G. // Nucl. Phys. B. 1977. V. 126. P. 298.
18. Dokshitzer Yu. L. // Sov. Phys. JETP. 1977. V. 46. P. 641.
19. Larin S. A., van Ritbergen T., Vermaseren J. A. M. // Nucl. Phys. B. 1994. V. 427. P. 41.
20. Larin S. A. et al. // Nucl. Phys. B. 1997. V. 492. P. 338; hep-ph/9605317.
21. Parente G., Kotikov A. V., Krivokhizhin V. G. // Phys. Lett. B. 1994. V. 333. P. 190; hep-ph/9405290.
22. Benvenuti A. C. et al. (BCDMS Collaboration) // Phys. Lett. B. 1987. V. 195. P. 91; 1989. V. 223. P. 485.
23. Rétey A., Vermaseren J. A. M. // Nucl. Phys. B. 2001. V. 604. P. 281; hep-ph/0007294.
24. Gorishny S. G., Larin S. A., Tkachov F. V. // Phys. Lett. B. 1983. V. 124. P. 217.
25. Gorishny S. G., Larin S. A. // Nucl. Phys. B. 1987. V. 283. P. 452.
26. Chetyrkin K. G., Tkachov F. V. // Nucl. Phys. B. 1981. V. 192. P. 159.
27. Larin S. A., Vermaseren J. A. M. // Phys. Lett. B. 1991. V. 259. P. 345.
28. Kataev A. L., Parente G., Sidorov A. V. // Proc. of Quarks-2000 Intern. Seminar, Pushkin, May 13–21, 2000. P. 53; CERN-TH/2000-343; hep-ph/0012014.
29. Dasgupta M., Webber B. R. // Phys. Lett. B. 1996. V. 382. P. 273; hep-ph/9604388.
30. Dokshitzer Yu. L., Marchesini G., Webber B. R. // Nucl. Phys. B. 1996. V. 469. P. 93; hep-ph/9512336.
31. Akhoury R., Zakharov V. I. Preprint UM-TH-97-05; hep-ph/9701378.
32. Beneke M. // Phys. Rep. 1999. V. 317. P. 1.
33. Beneke M., Braun V. M. Preprint PITHA 00/25; TPR-00-19; hep-ph/0010208.
34. Mankiewicz L., Maul M., Stein E. // Phys. Lett. B. 1997. V. 404. P. 345; hep-ph/9703356.
35. van Neerven W. L., Vogt A. // Nucl. Phys. B. 2001. V. 603. P. 42; hep-ph/0103123.
36. Yndurain F. J. // Phys. Lett. B. 1978. V. 74. P. 68.
37. Santiago J., Yndurain F. J. // Nucl. Phys. B. 2001. V. 611. P. 447; hep-ph/0102247.
38. Alekhin S. I., Kataev A. L. // Phys. Lett. B. 1999. V. 452. P. 402; hep-ph/9812348.
39. Alekhin S. I., Kataev A. L. // Nucl. Phys. A. 2000. V. 666–667. P. 179; hep-ph/9908349.
40. Alekhin S. I. // Eur. Phys. J. C. 1999. V. 10. P. 395; hep-ph/9611213.
41. Tarasov O. V., Vladimirov A. A., Zharkov A. Y. // Phys. Lett. B. 1980. V. 93. P. 429.
42. van Ritbergen T., Vermaseren J. A. M., Larin S. A. // Phys. Lett. B. 1997. V. 400. P. 379; hep-ph/9701390.
43. Floratos E. G., Ross D. A., Sachrajda C. T. // Nucl. Phys. B. 1977. V. 129. P. 66 (Erratum: Nucl. Phys. B. 1978. V. 139. P. 545).
44. González-Arroyo A., López C., Yndurain F. J. // Nucl. Phys. B. 1979. V. 153. P. 161.
45. Curci G., Furmanski W., Petronzio R. // Nucl. Phys. B. 1980. V. 175. P. 161.
46. Santiago J., Yndurain F. J. // Nucl. Phys. B. 1999. V. 563. P. 45; hep-ph/9904344.
47. Samuel M. A., Ellis J., Karliner M. // Phys. Rev. Lett. 1995. V. 74. P. 4380.
48. Kataev A. L., Starshenko V. V. // Mod. Phys. Lett. A. 1995. V. 10. P. 235; hep-ph/9502348.
49. Gardi E. // Phys. Rev. D. 1997. V. 56. P. 68; hep-ph/9611453.
50. Penin A. A., Pivovarov A. A. // Phys. Lett. B. 1996. V. 367. P. 342; hep-ph/9506370.

51. *Ellis J. et al.* // Phys. Rev. D. 1998. V. 57. P. 2665; hep-ph/9710302.
52. *Mikhailov S. V.* // Phys. Lett. B. 1998. V. 431. P. 387; hep-ph/9804263.
53. *Mikhailov S. V.* // Phys. Rev. D. 2000. V. 62. P. 034002; hep-ph/9910389.
54. *Broadhurst D. J., Kataev A. L., Maxwell C. J.* // Nucl. Phys. B. 2001. V. 592. P. 247; hep-ph/0007152.
55. *Korchemsky G. P.* // Mod. Phys. Lett. A. 1989. V. 4. P. 1257.
56. *Albino S., Ball R. D.* // Phys. Lett. B. 2001. V. 513. P. 93; hep-ph/0011133.
57. *Kotikov A. V., Maksimov S. I., Vovk V. I.* // Theor. Math. Phys. 1991. V. 84. P. 744 (Teor. Mat. Fiz. 1991. V. 84. P. 101).
58. *Ermolaev B. I., Greco M., Troyan S. I.* // Nucl. Phys. B. 2001. V. 59. P. 71; hep-ph/0009037.
59. *Kirschner R., Lipatov L. N.* // Nucl. Phys. B. 1983. V. 213. P. 122.
60. *Penin A. A., Pivovarov A. A.* // Phys. Lett. B. 1997. V. 401. P. 294; hep-ph/9612204.
61. *Sterman G.* Recent Progress in QCD // Plenary talk given at APS Meeting of the Division of Particle and Fields, Los Angeles, CA, Jan. 5–9, 1999; hep-ph/9905548.
62. *Dokshitzer Y. L.* Perturbative QCD and Power Corrections // Invited talk at 11th Rencontre de Blois: Frontiers of Matter, Chateau de Blois, France, June 28–July 3, 1999; hep-ph/9911299.
63. *Broadhurst D. J., Grozin A. G.* // Phys. Rev. D. 1995. V. 52. P. 4082; hep-ph/9410240.
64. *Brodsky S. J. et al.* // Phys. Rev. D. 1997. V. 56. P. 6980; hep-ph/9706467.
65. *Brodsky S. J., Lepage G. P., Mackenzie P. B.* // Phys. Rev. D. 1983. V. 28. P. 228.
66. *Ball P., Beneke M., Braun V. M.* // Nucl. Phys. B. 1995. V. 452. P. 563; hep-ph/9502300.
67. *Grunberg G., Kataev A. L.* // Phys. Lett. B. 1992. V. 279. P. 352.
68. *Rathsman J.* // Phys. Rev. D. 1996. V. 54. P. 3420; hep-ph/9605401.
69. *van Neerven W. L., Vogt A.* // Nucl. Phys. B. 2000. V. 568. P. 263; hep-ph/9907472.
70. *Chetyrkin K. G., Kniehl B. A., Steinhauser M.* // Phys. Rev. Lett. 1997. V. 79. P. 2184; hep-ph/9706430.
71. *Bernreuther W., Wetzel W.* // Nucl. Phys. B. 1998. V. 197. P. 228 (Erratum: Ibid. V. 513. P. 758).
72. *Larin S. A., van Ritbergen T., Vermaseren J. A.* // Nucl. Phys. B. 1995. V. 438. P. 278; hep-ph/9411260.
73. *Blumlein J., van Neerven W. L.* // Phys. Lett. B. 1999. V. 450. P. 417; hep-ph/9811351.
74. *Shirkov D. V., Sidorov A. V., Mikhailov S. V.* hep-ph/9707514.
75. *Shirkov D. V.* // Theor. Math. Phys. 1992. V. 93. P. 1403 (Teor. Mat. Fiz. 1992. V. 98. P. 500).
76. *Shirkov D. V., Mikhailov S. V.* // Z. Phys. C. 1994. V. 63. P. 463; hep-ph/9401270.
77. *Peterman A.* CERN-TH.6487/92.
78. *Brodsky S. J. et al.* // Phys. Rev. D. 1998. V. 58. P. 116006; hep-ph/9801330.
79. *Jegerlehner F., Tarasov O. V.* // Nucl. Phys. B. 1999. V. 549. P. 481; hep-ph/9809485.
80. *Kulagin S. A.* // Nucl. Phys. A. 1998. V. 640. P. 435; nucl-th/9801039.
81. *Kulagin S. A.* hep-ph/9812532.
82. *Kulagin S. A., Sidorov A. V.* // Eur. Phys. J. A. 2000. V. 9. P. 261; hep-ph/0009150.
83. *Webber B.* Private Communication. 1998.
84. *Martin A. D. et al.* // Eur. Phys. J. C. 2000. V. 18. P. 117; hep-ph/0007099.

85. *Schaefer S., Schafer A., Stratmann M.* // Phys. Lett. B. 2001. V. 514. P. 284; hep-ph/0105174.
86. *Bednyakov V. A. et al.* // Sov. J. Nucl. Phys. 1984. V. 40. P. 494 (Yad. Fiz. 1984. V. 40. P. 770).
87. *Kataev A. L., Starshenko V. V.* // Phys. Rev. D. 1995. V. 52. P. 402; hep-ph/9412305.
88. *Grunberg G.* // Phys. Rev. D. 1984. V. 29. P. 2315.
89. *Krasnikov N. V.* // Nucl. Phys. B. 1981. V. 192. P. 497 (Yad. Fiz. 1981. V. 35. P. 1594).
90. *Kataev A. L., Krasnikov N. V., Pivovarov A. A.* // Nucl. Phys. B. 1982. V. 198. P. 508 (Erratum: Nucl. Phys. B. 1997. V. 490. P. 505; hep-ph/9612326).
91. *Dhar A., Gupta V.* // Phys. Rev. D. 1984. V. 29. P. 2822.
92. *Maxwell C. J., Mirjalili A.* // Nucl. Phys. B. 2000. V. 577. P. 209; hep-ph/0002204.
93. *Matveev V. A.* Private Communication. 1981.
94. *Kotikov A. V., Parente G., Sanchez Guillen J.* // Z. Phys. C. 1993. V. 58. P. 465.
95. *Stevenson P. M.* // Phys. Rev. D. 1981. V. 23. P. 2916.
96. *Gorishny S. G. et al.* // Phys. Rev. D. 1991. V. 43. P. 1633.
97. *Chyla J., Kataev A. L., Larin S. A.* // Phys. Lett. B. 1991. V. 267. P. 269.
98. *Vermaseren J. A., Larin S. A., van Ritbergen T.* // Phys. Lett. B. 1997. V. 405. P. 327; hep-ph/9703284.
99. *Gardi E., Karliner M.* // Nucl. Phys. B. 1998. V. 529. P. 383; hep-ph/9802218.
100. *Bethke S.* // J. Phys. G. 2000. V. 26. P. R27; hep-ex/0004021.
101. *Hinchliffe I., Manohar A. V.* // Ann. Rev. Nucl. Part. Sci. 2000. V. 50. P. 643; hep-ph/0004186.
102. *Mangano M. L. et al.* Physics at the Front-End of a Neutrino Factory: a Quantitative Appraisal. Preprint CERN-TH/2001-131; hep-ph/0105155.